# Modelling effective brain connectivity using manifolds in optical functional neuroimaging

by

**Shender María Ávila Sansores**

Technical report CCC-16-006

Department of Computational Sciences

**National Institute for Astrophysics Optics and Electronics**
Tonantzintla, Puebla, México
January 15th, 2016

Supervisors:

**Dr. Felipe Orihuela Espina**
**Dr. Gustavo Rodríguez Gómez**
INAOE, México

# Abstract

The development of analytical approaches for decoding brain's effective connectivity from neuroimages remains open to improvement as existing model assumptions depart from physiological processes. Manifold based topological approaches are surprisingly underexplored considering the powerful mathematical abstraction they represent. This research hypothesizes that the brain function abides to the topological abstraction of a manifold, and thus the subsequent interactions among brain regions underpinning functional and effective connectivity can be expressed either as locations within the manifold or as trips along the manifold surface. In seeking to confirm this hypothesis, the aim is to develop a model of brain effective connectivity capitalizing on topological modelling of neurophysiological processes so that the connectivity network can retrieved from experimental neuroimaging data. As the physics of the image formation shall determine the topological characteristics of the dataset, the modelling will have to consider such modality-specific demands; in the case at hand, those of functional near infrared spectroscopy (fNIRS). To realize this goal, first the topological properties (continuity, differentiality and existence of a suitable metric) of the data will be characterized and the needs to represent the segregational response attended. It will be shown how the ambient Euclidean distance is insufficient for these purposes. Later, the integrational information will be univocally integrated within the direction of the flow of information first along a Riemann manifold by means of imposing a metric inspired on causal principles. Finally the inherent causal structure of certain manifolds such as the Lorentzian, will be harness to afford a computationally efficient modelling solution. Verification against synthetic scenarios and posterior validation against gold standard Dynamic Causal Modeling (DCM) over experimental observation will be carried out for the two modelling proposals. One important contribution in computational neuroscience of this thesis shall be the establishment of the foundations for topological modelling of brain function; an approach which has been hinted in literature but it is thus far lacking robust foundational mathematical support . Also, two major manifold-based modelling approaches i.e. Riemmanian and Lorentzian, will be explored. Finally, additional definition and establishment of topological constraints to be demanded to the resulting manifolds will be characterized so to ensure compliance with neurophysiological conditions and the exploitation of existing, or imposition of causal structure of manifolds to encode brain's effective connectivity. Successful completion of this research will provide new computational insights about topological modelling that should in principle be transferable to other domains, and it will further offer a new highly expressive causal modelling approach for one of the most important phenomenon to understand brain behaviour, effective connectivity.

## Keywords

topology, computational neuroscience, neuroimaging, effective connectivity, Riemannian manifold, Lorentz manifold.

# Contents

# Chapter 1

# Introduction

The field of *computational neuroscience* hypothesizes that all brain function can be explained algorithmically as the mere summation of information processing capabilities of the structures composing the nervous system. Although this foundational hypothesis has been seriously challenged by several authors including Penrose in his brilliant *The Emperor's New Mind* as ultimately unable to explain consciousness and the ability to think and have insight beyond algorithmic reasoning, Penrose himself as well as other critics recognise computational neuroscience as a pragmatic and highly successful theory for explaining the behaviour of such structures e.g. neurons, neural populations and neural networks, as well as many sub-phenomena of brain function and making inference about that function. In a sense, computational neuroscience stands in a similar position to relativity in physics which ultimately predicts its own downfall, but which is currently the best approximation to explain its domain.

Like relativity, computational neuroscience strongly requires causal models as some of the brain function phenomena are inherently causal e.g. effective connectivity. Relativity makes heavy use of topological modelling to support its causal expressions. Topology is the study of shapes and their deformations under continuous transformations. Central to topology is the concept of manifolds, locally flat surfaces that thus permit solving complex non-linear operations in curved surfaces by means of the recursive local application of a mathematical trick; local projection to a flat space, resolution of the operation in the flat space where our mathematical skills excel and then projecting back to the curved surface. The expression of causal relations within manifolds is often regarded as one of the most strict forms of causality Cox & Wermuth (2004), which perhaps explains its popularity in relativity.

The rationale of this research is that similar tools and methods from topology can be exploited in computational neuroscience to afford an encompassing model of brain connectivity. Brain connectivity regulates the brain's integrational working principle and has associative (functional connectivity) as well as causal (effective connectivity) sides, the latter being the matter of study here. The analogy with relativity is not far-fetched. Events in relativity's spacetime are alike neural firings. Transmission of

information in relativity is limited by speed of light and in the brain by the speed of electrical current. Causal influence is therefore restricted to events reachable within a certain cone deformed by mass and gravity in the case of relativity and by structural (anatomical) and metabolic (functional) constraints in the brain.

Departing from the hypothesis that the expression of brain function can be confined to a manifold, the present research aims to develop a new manifold-based modelling approach for the causal analysis of brain connectivity exploiting the expressive power of topology. Neuroimaging analysis in terms of topological manifolds consist of encapsulating the solution space of the system's response i.e. brain activity interrogated by means of some neuroimaging technique, within a (hyper)-surface described by a collection of local charts, globally defining an atlas. The individual charts, describing open subsets, exploit the unique characteristics inherent to manifolds.

The image formation and reconstruction differs among neuroimaging modalities which imply that the glass through which the brain function is observed deforms the observations in rather distinct ways depending on the neuroimaging modality. Such deformation of the topological properties of the observation has to be taken into account during the modelling process and ultimately affect the computational limitations of the modelling solution. For the purposes of this research, the study of effective connectivity will be attempted from the functional optical imaging technique known as functional near-infrared spectroscopy (fNIRS).

Resulting from this research, two modelling approaches of brain's effective connectivity based on the Riemann and Lorentzian manifolds are expected, and the computational implications (advantages and limitations) of both approaches will be established.

The distribution of solutions, topology of these, in the solution space problem affects computability thereof. In this sense, so that a problem is well posed, Hadamard requires that these solutions (i) there, (ii) are unique for a given input and (iii) vary smoothly with respect to the input. The latter requirement is strictly topological and implies that the topology of the solutions should be differentiable. Study the topology of the solutions, such as deciding whether a Riemannian or Lorentzian surface is suitable and under what conditions to describe this topology, is therefore a central issue in computing.

## 1.1 Motivation

Manifolds are now a common analytical tool for scientists across diverse fields such as genetics, robotics and biomedical imaging among others Lee (2012). In the field of interpretations of functional neuroimaging is still rudimentary, especially considering the expressive power offered by this type of modeling to encode and retrieve causal relations Krym (2002); Rainer (1999). Thus far in this field, the existing work has mainly focused on the application of concepts obviating the formalization of those concepts, as these involve exploiting the intrinsic properties of the surfaces do Carmo (1976); Berger & Gostiaux.

In computational neuroscience, a number of functional neuroimaging modalities allow the neuroscientific community to routinely ask questions about the brain behaviour *in vivo*. As these neuroimaging have become more refined so have the questions that the neuroscientists pose and so the greater are the challenges of computational neuroscience to afford models to fit the observations. Computational, statistical and in general, mathematical models from naive to elaborated have been the supporting language to express the different hypothesis about brain structure and function with an exciting overall performance, both predictive and explicative. For instance, we now have models for explaining the mechanisms to detonate axon potentials like the well-known Hodgkin-Huxley and its offsprings Abbott & Kepler (1990); Toral *et al.* (2003), for encoding the hemodynamic response to brain activation Buxton *et al.* (2004), for expressing functional Ng *et al.* (2014) and effective connectivity Friston *et al.* (2003), etc. And yet, none of these models seems encompassing enough to express the broad range of brain function phenomena; segregational and integrational, transversal and longitudinal, direct (neural) or indirect (haemodynamic), associative or causal, etc. Perhaps one of the reasons is that given the complexity of brain behaviour it has been thus far more practical to think (and address) one phenomenon at a time.

Even with this atomization of the problem, in the particular case of effective connectivity, central to this research, the causal demand and the systematic departure of model assumptions from neurophysiological truths leaves a clear margin for improvement. Certainly, we know the problem is ill-posed, but most times even the most basic computational properties of the problem are ignored leaving a huge gap in our knowledge.

## 1.2 Justification

Understanding how the human brain works is arguably one of the biggest challenges of the twenty-first century science. With this knowledge it shall be possible to develop new treatments for brain disorders, improve diagnosis, build communication technologies not mediated by regular sensorial channels, introduce advances in robotics, afford novel bioinspired artificial intelligence solutions, etc. The study of cerebral connectivity Bassett & Bullmore (2006); Bullmore & Sporns (2009) deepens the understanding of brain function. Methodologies to detect and quantify the different types of connectivity directly impact our ability for diagnosis and treatment of various neurological and mental conditions. Neuroimaging techniques are now a major area of study in understanding the brain's pathophysiology.

For definition the analysis of effective connetctivity demand a causal model. The actually effective connectivity models for example dynamic causal modelling o structural equation modelling are contruction on a asociative model limited of expresion causal. The causal models extructuration of Cox Cox & Wermuth (2004), the topological models based of manifold are a tool with which we have to express causal relationships. Perhaps proof of this is of supports model of the theory of relativity where there is also an

inherent requirement of causal models. In other words, based on modeling manifold has the potential to support a causal expressions.

And by means of the computational neuroscience foundational hypothesis the study of brain behaviour and computing are tightly interlinked. Indeed, subfields such as *neurocomputing* the computational modelling of the nervous system structures, *neuroinformatics* organization of neuroscience data by the application of computational models and analytical tools and *neural computation* development of neurally inspired models for computing among others are hectic areas of research.

## 1.3 Problem statement

This work addresses the problem of revealing effective (causal) relations describing the interplay among hidden system entities i.e. brain regions, when responding to a certain task from a set of indirect observations i.e. superficial optical measurements encoding brain haemodynamics as a proxy of brain activity. The latent computational problem of modelling causal relation over unobserved variables from their indirect consequences remains open. This problem is currently being attacked from different approaches Pearl (2009); Lamport (1978) etc. One of the approaches, closer to the topological attempt proposed in this research is perhaps manifold learning Cayton (2005), but this seem to have thus far seen better success in associative modelling.

The problem is essentially how to maintain; so that they can be later retrieved, causal relations across a composition of several functions deforming the space of interest. Given that both the neural response function and the hemodynamic response function, although spatiotemporally non-linear Sheth *et al.* (2004),Sheth *et al.* (2005), are often regarded as continuous and differentiable, the problem is expressed as a topological one, where the space of solutions lays on a locally linear hypersurface (or manifold). A bit more formally, given a set $O$ of superficial optical measurements at a number of locations (or channels) $i$, recover the manifold $M$ where each point in the surface of the manifold represents a global or partial solution in the configuration space.

This is in fact a multistage mapping (indeed we intend to show that structures are respected across the transformations).

$f : N \times C \rightarrow H \rightarrow OP \rightarrow O$

where $N$ represents the space of neural activity often expressed by regions, $C$ represents the connectivity space whether functional or causal, $H$ represents the haemodynamic space normally affected by noise such as the systemic, $OP$ is the space of optical properties of the head tissues and $O$ is the space of optical measurements at scalp. The submappings $N \rightarrow H$[1], $H \rightarrow OP$ and $OP \rightarrow O$ are often referred to as the neural activation model, the haemodynamic response model and the image reconstruction model respectively. As it will discussed all of these functions have received extensive attention

[1]Note the absence of the connectivity space.

by their own. The overall problem of recovering the connectivity configuration $C$ is an inherenty ill-posed problem with many possible brain configurations raising the observed optical functional neuroimage.

In addition to the existence of multiple solutions, it is unclear how these solutions are to be represented mathematically to make neurophysiological sense, what it is referred here as the semantics of the representation. Here, the semantics of a mathematical representation refers to the physiological construct being encoded. The semantics of the representation is also open to multiple options. For instance, a point in a space may represent a full solution i.e. the whole graph (topology) of brain connectivity, whether functional or effective, an approach commonly chosen when manifolds are the tool chosen for representing the solution space of a problem. Alternatively, a point in a space may only partially encode the local behaviour of the brain at a certain region or channel, and it is a path along the manifold which describes the flow of information across regions, i.e. a solution.

None of the specific submappings may have specific relevance to our modelling strategy, but their effects will be noted in the different deformations that they introduced. Consequently their choice has computational implications.

The first encodes causal relationships as a direct consequence of the location of each point on the array where the direction of the relationship is encoded by the negative signature of the metric tensor and uses the causal structure of the variety itself (ie, manifold causal). The second alternative encodes causal relationships as a displacement on the variety in what is known as a world-line. This second approach works on manifold of positive signature and therefore the variety lacks a causal structure as such, which is imposed externally by imposing a pseudo-metric to discern the direction of travel on the variety. During the thesis, we hope to elucidate the advantages and limitations of each of these representations.

Finally, the demand of expressing causality precludes classical associational models from giving a satisfactory response to the problem. The appreciation of the causal relations among system entities shall be attempted by imposition of a causally inspired distance function over the manifold, and by exploitation of causal manifolds inherent structure.

## 1.4 Research questions

1. Does the segregational behaviour of the system i.e. the brain, fits the mathematical abstraction represented by a manifold? In other words, do the physical characteristics of the problem domain, that of neural activation match the topological characteristics of the manifold?

   *Disambiguation:* Before addressing the integrational questions, i.e. those of connectivity ruling the collaborative behaviour among brain regions, it is necessary to show that the segregational behaviour of the brain, i.e. localised specialized

activity, is susceptible to be expressed by means of the topological abstraction of a manifold. As it will be discussed, early work Friston *et al.* (1996); Leff *et al.* (2007) assumed this to be the case and retrieves neuroimaging interpretations with certain nomological validity, thus suggesting this relation between the segregational construct and the topological abstraction might be plausible. However, evidence, whether analytical or experimental of this assumed relation is lacking.

*Purpose:* The purpose of this question is to identify the topological properties (continuity, differentiality, and existence of a distance function) needed to represent the segregational response, and in turn determine the manifold that suits these mathematical demands, which it is expected to be the Riemmann manifold.

*Assessment of success:* Answering this question involves both analytical work over existing forward models e.g. check continuity in specific haemodynamic response models, and experimental work e.g. observing the distribution of locations expressed in the manifold subsequent to a particular stimulation of the brain, and checking that it is possible to define a path among these locations without violating any physiological constraints considered. The specific demands to the cascade of transformations have to be stated. Their impact on the computability of the solution has to be established.

2. Under which topological restrictions an imposed metric over the Riemann manifold does capture integrational (functional) features of the activity of the system entities i.e. brain regions? And how these topological restrictions do arise from known problem domain i.e. neurophysiological, constraints?

   *Disambiguation:* Moving to integrational relations among system entities, being embedded in a space of positive signature it is known that paths along the Riemann manifold without any further constraints are unable to represent directionality of the information flow, and thus only functional (associative) but not effective (causal) aspects, can be encoded in the default manifold. However, it is conceivable that imposing additional topological restrictions to the manifold, such as an asymmetric distance function, can be harness to encode causal relations among different manifold loci, hence travelling along the manifold can be restricted to only those paths encoding pseudo-causal spatiotemporal relations. This question, assumes a positive finding in the first question i.e. some manifold within a positive signature ambient space can encode segregational aspects of brain activity. The particular case of a Riemann manifold is secondary, with other topological abstractions also being possible. The question is however expressed in terms of the Riemman manifold to reduce ambiguity.

   *Purpose:* The purpose of the question is to establish an univocal direction for the flow of information along a Riemann manifold. Since precedence is a necessary (but not sufficient) condition for expressing causality, the natural geodesic metric has to be abandon and a directional distance function where $d(x, y) \neq d(y, x)$ is

required. The compromise of relaxing any original metric might be obvious from the mathematical point of view, but it is far from clear what the subsequent space deformation does represent in physiological terms and its computational impact. It may be the case that the pseudometric imposed has to consider the particular semantics being encoded in the manifold.

*Assessment of success:* Answering this question requires analyzing the deformation suffered by the manifold whenever a new distance function is imposed. Some deformations are known in advance; e.g. imposing a 1-correlation pseudometric projects to a hypersphere, but others, depending on the function are not. This first analysis can be done either analytically or empirically from synthetic data. But understanding the implications that the deformation has in physiological terms can only be inferred from experimental interrogation. The same experiment carried out to answer the first question can be further exploited here, and there is only need for an additional analysis. Successful recovery of synthetic truths will be considered sufficient to answer this question.

3. Under which conditions can the expressive power of causal manifolds, such as the Lorentzian, be harness to express causal integrational (effective) relations among system entities?

   *Disambiguation:* Progressing to a space of negative signature, certain manifolds already incorporate a causal structure thus enabling the exploration of causal integrational (effective) relations among brain regions. Hence analogous to the first question, we formulate again the the interrogation regarding whether the domain i.e. neurophysiological, construct does obeys the mathematical demands of the chosen abstraction. This is far from trivial; getting into the unfamiliar world of negative signature spaces gives new unsuspected meanings to familiar concepts. Distance functions, for instance, can now yield negative values denoting precedence. The geodesic along the manifold may again suffice to express the physiological construct given the adequate semantics.

   *Purpose:* The purpose of this question is three-fold. First, the mathematical rigour has to be complied with, in a sense analogous to the first question. Second, these mathematical concepts have to be reinterpreted according to the physiological construct and still be meaningful. Third, assumptions computationally valid in positive signature spaces may no longer hold in negative signature spaces and thus have to be reassessed.

   *Assessment of success:* Answering this question requires a procedure similar to that applied to answer the first question. Again analytical and experimental work is required, and again, data from the first experiment can be reused to achieve nomological validity. Only interpretation is updated within the new mathematical framework. Sucess will be claimed if concurrent validity against the current gold

standard for the analysis of effective connectivity, dynamic causal modelling can be established.

## 1.5 Hypotesis

The naked computational hypothesis is that the retrieval of causal relations in a manifold when the manifold has been severely distorted through a chain of (non-linear) transformations is a computationally feasible task as long as certain properties are maintained through the deformations and such deformations are properly understood.

The analogous computational neuroscience hypothesis follows; If brain function abides to the topological abstraction of a manifold, then the associated and causal relations underpinning functional and effective connectivity can be expressed either as trips along the manifold surface, or as full solutions captured at points in the manifold

### 1.5.1 Aim

The general aim of the research is to afford the development and assessment (verification and validation) of a new topological approach for the modelling and retrieval of causal relations among system entities while affording complex tasks from the observation of indirect markers of the individual activity by the specialized entities. This problem mimics the requirements of the neurophysiological phenomenon of brain's effective connectivity when such neurophysiological phenomenon is interrogated by fNIRS neuroimage

Specific goals are:

- Analysis of the topological properties demandable to the cascade of transformations involved in the indirect observation of the phenomenon. In the domain at hand, this includes the neural and hemodynamic responses as well as the image formation and reconstruction processes.
- Establishment of the adequacy of an existing distance function or development of an appropriate distance function under which a manifold within a positive signature space encodes the pseudo-causal relations. In computational neuroscience this equates to express (pseudo-)effective connectivity.
- Exploitation of the causal manifolds expressive power and characterization of the computational assumptions to be held.
- Concurrent and nomological validation of the proposed modelling approaches.

## 1.6 Assessment and scope

This research focuses on the development of the computational modelling approach for guaranteeing successful retrieving of causal relations in topological spaces i.e. manifolds.

The domain of application is the modelling of brain's effective connectivity. Although the thesis is inherently multidisciplinary requiring knowledge related to neuroscience, calculus, linear algebra and topology, this research will be on the development of algorithms that permits encode the causal structure of manifolds.

## 1.7 Contributions

The main contributions of this research are expected to be the following:

- Exploration of how causal relations within a manifold are (or can be) maintained through a number of non-linear deformations in terms of the topological properties demanded.
- Foundations for topological modelling of brain function will be established
- Definition and establishment of topological and computational constraints to the built manifolds to ensure (i) compliance with domain conditions, and (ii) feasibility of the computability of the solution.
- Exploitation of existing, or imposition of, causal structure of manifolds to encode brain's effective connectivity

## 1.8 Chapter summary

This chapter aimed to provide the reader with an overview of the intended research. Major elements of science and the scientific method, such as the research questions and hypothesis, the goals and expected contributions and the significance and rationale of the research have been put forth. The rest of the document provides theoretical and referential support as well as preliminary evidence to the feasibility of the enterprise. Also intended methodology is further detailed.

# Chapter 2

# Background

In this section, the notation and some basic definitions needed to understand the following sections are given.

## 2.1 Basic definitions

Some notation is introduced:

1. Let $\mathbb{R}$ be the set of real numbers. If $n$ is a positive integer, then

$$\mathbb{R}^n = \underbrace{\mathbb{R} \times \mathbb{R} \times \ldots \times \mathbb{R}}_{n-\text{times}},$$

   is the set of all $n-$tuples of real numbers. Thus, if $a \in \mathbb{R}^n$

$$a = (a_1, \ldots, a_n), \;\; a_i \in \mathbb{R}.$$

2. For $u_i$, $i = 1, 2, \ldots n$, let $u_i$ be the natural coordinate (slot) functions of $\mathbb{R}^n$, i.e., $u_i : \mathbb{R}^n \to \mathbb{R}$ by $u_i(a_1, a_2, \ldots, a_n) = a_i \in \mathbb{R}$.

3. Let $a = (a_1, a_2, \ldots, a_n)$ and $b = (b_1, b_2, \ldots, b_n)$ be two points in $\mathbb{R}^n$. We defined

$$d(a, b) = \left[ \sum_{i=1}^{n} (a_i - b_i)^2 \right]^{\frac{1}{2}},$$

   and is called the Euclidean distance.

4. Let $x$ be a point in $\mathbb{R}^n$ and $\epsilon > 0$ a radius, then $\epsilon$ defines a **neighorhood** of $x$ as $V_\epsilon(x) = \{y \in \mathbb{R}^n | d(x, y)| < \epsilon\}$

5. Let $X$ be a set, by $2^X$ we mean the set of all subsets of $X$, which is called the **powerset**.

6. Let $f$ be a function $f : (a, b) \to \mathbb{R}$. The function $f$ is continuous at the point $x_0$ if

   - $x_0 \in (a, b)$ i.e. $x_0$ belongs to the domain of $f$
   - $f(x_0) \in \mathbb{R}$
   - $\lim_{x \to x_0} f(x)$ exists, and
   - $\lim_{x \to x_0} f(x) = f(x_0)$

7. Let $S$ and $S'$ be two set. A **map** from $S$ to $S'$ is a continuous function $f : S \to S'$

8. Let $\mathbb{K}$ be a subset of the complex numbers $\mathbb{R}$ or $\mathbb{C}$. $\mathbb{K}$ is a **field** if it satisfies the following conditions:

   - If $x, y \in \mathbb{K}$, then $x + y$ and $xy$ are also elements of $\mathbb{K}$
   - If $x \in \mathbb{K}$, then $-x$ is also an element of $\mathbb{K}$. If furthermore $x \neq 0$, then $x^{-1}$ is an element of $\mathbb{K}$.
   - The elements 0 and 1 are elements of $\mathbb{K}$

9. Consider $\mathbb{R}^4$ and let $\{e_1, e_2, e_3, e_4\}$ be the canonical basis. If $x = (x_0, x_1, x_2, x_3)$, $y = (y_0, y_1, y_2, y_3)$ are points in $\mathbb{R}^4$, then the scalar product defined by

   $$\langle x, y \rangle = -x_0 y_0 + x_1 y_1 + x_2 y_2 + x_3 y_3,$$

   is called the Minkowski metric. It can be proved that Minkowski metric signature is given by (-1,1,1,1);

10. The restriction of a function $f$ is a new function $f|_A$ obtained by choosing a smaller domain $A$ from the original function $f$.

11. A function $d : S \times S \to \mathbb{R}$ is called a **metric** on $S$, if for every set of points $s_1, s_2, s_3 \in S$ it satisfies the following

    (a) $d(s_1, s_2) > 0$ if $s_1 \neq s_2$, $d(s_1, s_1) = 0$

    (b) $d(s_1, s_2) = d(s_2, s_1)$

    (c) $d(s_1, s_3) \leq d(s_1, s_2) + d(s_2, s_3)$

    Then the pair $(S, d)$ is called a **metric space**, where $S$ is a non-empty set and $d$ is a metric. If instead of property (a) the function satisfies (a'): $d(s_1, s_2) = 0$ if $s_1 \neq s_2$ then the distance function $d$ is called a **pseudo-metric**.

12. Let $A \subset \mathbb{R}^n$ be an open set and $f$ a real-valued function $f : A \subset \mathbb{R}^n \to \mathbb{R}$, then it is said that $f$ is a map of **differentiable class** $r$ **on** $A$ with $r \in \mathbb{N}^+$, and denoted $C^r(A)$, if it possesses continuous partial derivatives on $A$ of all orders $r$.

a If $f$ is merely continuous in $A$ (it has no derivatives) then $f$ is of class $C^0$ on $A$.

b If $f$ is real and analytical[1] of $A$, then $f$ is of class $C^\infty$ in $A$, and it is said to be **smooth**.

## 2.2 Spaces

**Definition 2.2.1.** An $\mathbb{R}^n$ is a **Euclidian space** if its metric (distance function) is the Euclidean distance.

**Definition 2.2.2.** A **vector space** $V$ over the field $\mathbb{K}$ is a set of objects which is defined by two maps:

- a map $(x, y) \to x + y$ from $V \times V$ into $V$ called *addition*
- a map $(\lambda, x) \to \lambda y$ from $\mathbb{K} \times V$ into $V$ called *multiplication by a scalar*

These maps (or algebraic operations) must satisfy the following axioms:

1. $x + y = y + x$ commutativity
2. $(x + y) + z = x + (y + z)$ associativity
3. There exists an element 0 in $V$ such that $x + 0 = x$ for all $x \in V$. This element 0 is called the *zero vector*.
4. For every element $x \in V$, there exist an element $-x \in V$ such that $x + (-x) = 0$. The element $-x$ is called the *opposite* of $x$.
5. $\lambda(x + y) = \lambda x + \lambda y$
6. $(\lambda + \mu)x = \lambda x + \lambda\mu$
7. $(\lambda\mu)x = \lambda(\mu x)$
8. $1\dot{x} = x$ for all $x \in V$

The elements of a vector space are called *vectors*

**Definition 2.2.3.** Let $E$ be a finite dimensional vector space finite dimensional. A **symmetric bilinear form** on $E$ is an application $\mathbb{R}-$bilinear $g : E \times E \to \mathbb{R}$ such that $g(u, v) = g(v, u)$ for all $u, v \in E$. If $g$ further satisfies the following condition

[1] A function is analytic if and only if its Taylor series about $x_o$ converges to the function in some neighborhood for every $x_o$ in its domain.

i) $g(u,u) > 0 \ \forall\, u \neq 0$, $g$ is called positive definite

ii) $g(u,u) < 0$ for all non zero vector $u \in E$, $g$ is called negative definite

iii) $g(u,u) = 0 \ \forall\, v \in E$, implies $u = 0$, $g$ is called nondegenerate.

We use the following notation interchangeably $g(u,v) = \langle u, v\rangle$.

**Definition 2.2.4.** A **topology** in $X$ is a nonempty collection $\tau \subseteq 2^X$ of subsets of $X$ called open sets, which satisfy the following four axioms:

1. The empty set $\emptyset$ is open
2. The set $X$ itself is open
3. The union of any family of open sets is open
4. The intersection of any two ( and hence of any finite number of) open sets is open

The pair $(S, \tau)$ is called **topological space**.

**Definition 2.2.5.** Let $g : E \times E \to \mathbb{R}$ be a bilineal symetric form. The index $\nu$ of $g$ is the integer positive number that is the dimension of the largest subspace $F \subset E$, on which $g|_{F\times F}$ is negative definite. Where $g|_{F\times F}$ means the restriction function of $g$ on $F \times F \subset E \times E$. It should be observed $0 \leqq \nu \leqq n = \dim(E)$ and $\nu = 0$ if and only if $g$ is positive definite.

**Definition 2.2.6.** A scalar product $g$ on a vector space $E$ is a nondegenerate symmetric bilinear form. For example, if the scalar product is also positive definite is called **inner product**.

**Definition 2.2.7.** Let $E \neq \{0\}$ be a vector space with a scalar product $g$ and consider the associated diagonal matrix $D$ of $g$ relative to an orthonormal basis. The diagonal elements of $D$, denoted by $(\varepsilon_1, \ldots, \varepsilon_n)$, is **the signature of g**.

**Definition 2.2.8.** If $X$ and $Y$ are topological spaces, a **homeomorphism** from $X$ to $Y$ is a bijective map $\varphi : X \to Y$ such that both $\varphi$ and $\varphi^{-1}$ are continuous. If there exists a homeomorphism between $X$ and $Y$, say that $X$ and $Y$ are homeomorphic or topologically equivalent.

**Definition 2.2.9.** The couple $(\mathbb{R}^4, \langle\ ,\ \rangle)$, where $\langle\ ,\ \rangle$ is the Minkowski metric, is called Minkowski space.

**Definition 2.2.10.** An **event** is something that happens instantaneously at a single point in Minkowski space.

# Chapter 3

# Theoretical Basis

The manifolds are topological spaces than locally "look the same" as Euclidean spaces. Every point of a topological manifold has an neighborhood in which we can establish a mapping (coordinate system) to an open subset of $\mathbb{R}^n$. This fact allow us use concepts of $\mathbb{R}^n$ on manifolds at least locally (that is, at least for each neighborhood) Guillemin & Pollack (2010),(Guillemin & Pollack, 2010). A manifold can be considered as an object composed of open subsets that "look the same" as open subsets of $\mathbb{R}^n$. Some examples are showed in Figure 3.1. In Figure 3.2 is depicted a topological region that is not a manifold.

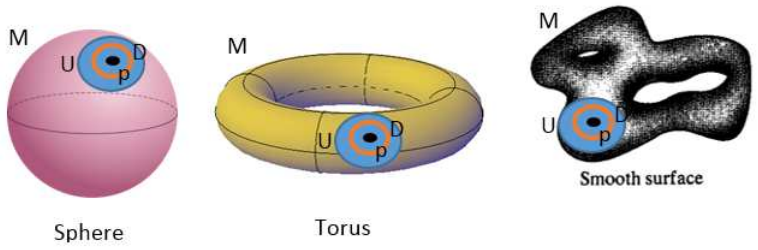


Figure 3.1: Manifolds examples. $U \subseteq M$ is a neighborhood of point $p \in M$, if there is a disk $D$ such that $p \in D \subseteq U$ then is possible a map to $\mathbb{R}^n$. Figure reproduced from (Guillemin & Pollack, 2010)

## 3.1 Differentiable manifolds

Before giving the formal definition of a manifold, first some concepts is introduced. Let $V$ be a Euclidean space and $M$ a subset of $V$. A $V-$**atlas of class** $C^k$ on $M$ is a

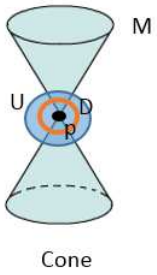


Figure 3.2: Example of a shape that is not a manifold. The cone in the example is not a manifold because there is no arbitrary neighborhood around the vertex point which is contained within the cone. In other words, there are points in D that are not in M. Figure reproduced from (Guillemin & Pollack, 2010)

collection $a$ of pairs $(U_i, \phi_i)$ called **charts**, where $U_i$ is a subset of $M$ and $\phi_i$ is a bijective map of $U_i$ onto an open subset of $V$ subject to the following conditions (Figure 3.3):

**A1.** For any $(U_i, \phi_i) \in a$ and $(U_j, \phi_j) \in a$ the sets $\phi_i(U_i \cap U_j)$ and $\phi_j(U_i \cap U_j)$ are open subsets of $V$, and the maps

$$\phi_i \circ \phi_j^{-1} : \phi_j(U_i \cap U_j) \to \phi_i(U_i \cap U_j)$$

are differentiable of class $C^k$.

**A2.** $\bigcup U_i = M$.

The functions $\phi_i \circ \phi_j^{-1}$ are called the **transition functions** os the atlas $\mathbf{A}$.

Let $\mathbf{A}_1$ and $\mathbf{A}_2$ be atlases on $M$. We say that they are equivalent if their union $\mathbf{A}_1 \cup \mathbf{A}_2$ is again an atlas on $M$.

**Definition 3.1.1.** A set $M$ toghether with an equivalence class of atlases on $M$ is called a **differentiable manifold**.

**Definition 3.1.2.** Let $M$ be a manifold of class $C^\infty$ and $m \in M$ a point on the manifold. The **tangent vector** $X$ is a function $X \in C^\infty(m)$ such that it satisfies the following: f,g $\in C^\infty(m), b \in \mathbb{R}$

1. $X(f+g) = Xf + Xg$
2. $X(bf) = b(Xf)$
3. $fg = (Xf)g(m) + f(m)(Xg)$

Where $C^\infty(m)$ is the set of real valued function that are on some neighborhood of $m$.

**Definition 3.1.3.** The **tangent space** to $M$ at $m \in M$, denoted by $T_m(M)$, is the set of all tangent vectors at $m \in M$.

The tangent space $T_m(M)$ is a vector space over $\mathbb{R}$.

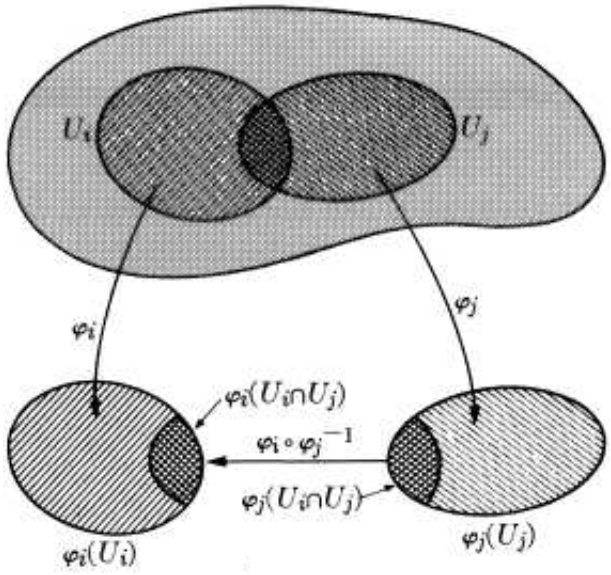


Figure 3.3: An n-coordinate pair $(U, \varphi)$ on $M$ is called a chart. $\varphi$ is a homeomorphism $\varphi : U \subset M \to \mathbb{R}^n$ onto an image $V = \varphi(U)$ which is an open set in Euclidiean space. Figure reproduced from (Loomis & Sternberg, 1968).

## 3.2 Riemmannian manifold

**Definition 3.2.1.** A Riemmannian manifold is a $C^\infty$ manifold $M$ on which one has singled out a $C^\infty$ real valued, bilinear, symmetric, and positive definite function $\langle\ ,\ \rangle$, on ordered pairs of tangent vectors at each point. Thus if $X, Y$ and $Z$ are in $M$, then $\langle X, , Y, \rangle$ and is a real number and $\langle\ ,\ \rangle$ satisfies the following properties Hicks (1965) Thorpe (1994):

a) Symmetric. $\langle X, Y\rangle = \langle Y, X\rangle$

b) Bilinear. $\langle X + Y, Z\rangle = \langle X, Z\rangle + \langle Y, Z\rangle$ and $\langle aX, Y\rangle = a\langle X, Y\rangle$ for $a$ in $\mathbb{R}$

c) Possitive definite. $\langle X, X\rangle > 0$ for all $X \neq 0$

**Definition 3.2.2.** When $c$) is replaced by c') For all $X$, $\langle X, Y\rangle = 0$ implies $Y = 0$ then $M$ is a **semi-Riemannian** (or **pseudo-Rimannina**) **manifold**.

In either case, the function $\langle\ ,\ \rangle$ is the metric tensor. Notice the word "metric" is not referring to a metric function (distance function) in the topological sense. The metric tensor will allow us define lengths, angles and distances.

## 3.3 Lorentzian Manifold

**Definition 3.3.1.** A pseudo-Riemannian manifold is called Lorentzian manifold if $g$ has signature $(-1, 1, \ldots, 1)$.

## 3.4 Manifolds as causal spaces

The relation of causality between points on the manifold is studied as models of space-time often within pseudo-Riemannian manifolds. Mathematically the concept of a space-time in a pseudo-Riemannian manifold are described with coordinate systems that have three spatial dimensions and one temporal dimension. It is impossible to picture a four-dimensional space, and thus it is common to make use of space-time diagrams (also known as Minkowski diagrams), where there is (usually) a vertical time axis and a horizontal spatial $x$ axis.

The set of all events that occurred, are occurring or will occur in the universe at any given time is called the **Space-Time**. The motion of a particle is represented by a trajectory in the space-time. A possible analogy with brain function arise naturally; the particle may represent a neural firing at certain brain location which is transmitted (it travels along the space-time manifold) to another brain region.

In order to describe the notion of causal and chronological precedence on semi-Riemannian manifold, is necesary to have two partial orderings: the causality relation denoted by $\prec$ and the chronology $\ll$. An event $x$ causally precedes an event $y$ if the interpretative principles would allow an occurrence at $x$ to influence what happens at $y$, or if a message could be transmitted from $x$ to $y$. The chronological precedence corresponds to the possible time-ordering of events on the world-line of an idealized observer whose velocity is less than that of light (see Kronheimer & Penrose (1967); Bombelli *et al.* (1987); O'neill (1983)).

## 3.5 Brain connectivity

The brain function abides by two fundamental principles: segregation and integration Frackowiak *et al.* (2004); Zamora-López *et al.*. The principle of segregation or specialization refers to the organization of neurons in specialized groups distributed in different regions of the cerebral cortex i.e. different regions of the brain taking responsibility for specific basic fundamental tasks whether sensorymotor or cognitive, whereas the functional integration is the mechanism that leads to the coordinated activation of the segregated brain Friston (1994) tag (2004) permitting the execution of more complex tasks. Functional integration refers to the interactions among specialised neuronal populations and how these interactions depend on the sensorimotor or cognitive context. The

study of functional integration is carried out majorly through three types of connectivity (Horwitz, 2003):

- **Anatomical or structural connectivity** referring to the study of physical connections among neural populations
- **Functional connectivity** defined as a associative dependence of neuronal activity between anatomically separate brain regions
- **Effective connectivity** that concerns the causal influence that a brain region exerts over another, either at a synaptic or population level.

Functional connectivity is the manifestation of the phenomenon of integration that dictates how different brain regions work together to carry out certain tasks. Depending on the type of collaboration that can be quantified by statistical dependence, correlation, coherence etc. The type of collaboration can be a simple co-activity (which for example allows us to do more than one task "while"), or require specific coordination between several regions (which for example allows us to perform complex tasks). Both types of connectivity are required; the first is the functional (or merely associative) connectivity, and the second is known as effective (or causal). In other words, while the functional connectivity is trying to explain the associative units, in effective connectivity directed causal influence between brain regions analyzed.

### 3.5.1 Brain activity

When a neuron fires a number of effects occur in the neuron and its surroundings. These effects allow different imaging techniques to observe the brain function, either directly or indirectly.

The nervous system transmits the information by means of electrical signals. The **action potential** is a temporary change in electrical potential across the neuron membrane, from negative to positive and then back to negative (Bear *et al.*, 2007; Kandel *et al.*, 2000) that permits the neuron either to initiate an activity or to pass incoming information. Neurons at rest stores a voltage of about $-65mV$,. When the neuron activates, an exchange of sodium (Na +) and potassium (K +) ions through the membrane of neurons alters the voltage to produce an electrical impulse of approximately $38mV$ (the action potential). The electrical signature of the neuron firing is illustrated in Figure 3.4.

The neuron metabolic activity enabling the neuron firing requires oxygen. The **neurovascular coupling** is the process regulating the coupling between neuronal activity (energy demand) and local blood flow (energy supply) Rosengarten *et al.* (2001). As the neuron becomes active, it starts consuming the oxygen in its surroundings producing a transient increase of reduced haemoglobin which is quickly followed by the flooding of the brain region with oxygenated blood leading to the characteristic increase in the

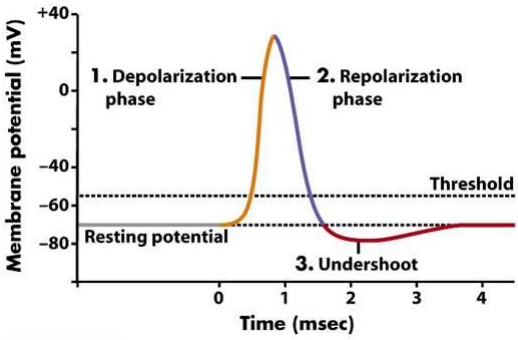


Figure 3.4: The action potential is a redistribution of electrical charge across the neuron membrane. Depolarization of the cell during the action potential is caused by the influx of sodium ions across the membrane, and repolarization is caused by the efflux of potassium ions. This process occurs within a timeframe of 10ms including the neuron refraction period. Figure reproduced from: *http* : *//www.uic.edu/classes/bios/bios*100/*lectures/action_potential.jpg*

concentration of oxygenated hemoglobin (HbO2) and the decreased of the deoxygenated hemoglobin (Hb) Leff *et al.* (2011); Meek *et al.* (1995). The approximate time of the transient stage from the start of neuronal activity and the flooding of HbO2 is approximately 3-5s. The characteristic waveform of the blood oxygenation level dependent (BOLD) hemodynamic response Kamran *et al.* (2015) Çiftçi *et al.* (2008) is show in Figure 3.5 .

In the literature there are several models that approximate the hemodynamic response such as that of Buxton *et al.* (2004) where brain haemodynamics is expressed in terms of the familiar quantities: Cerebral blood flow (CBF), Cerebral blood volume (CBV) and Cerebral metabolic rate of oxygen (CMRO2), or modeled to a summation of gamma variate functions whose parameters are optimized experimentally to form a canonical hemodynamic response function (HRF) Friston *et al.* (1998). Other physiological phenomena that are sometimes included in the model is the systemic response including for example noise, heartbeat and breathing among others Diamond *et al.* (2006); Zhang *et al.* (2005) among others.

## 3.6 Functional near-infrared spectroscopy (fNIRS)

One way to study the brain function is by means of functional neuroimaging [1] which permits examination of the human brain in vivo noninvasively. Different neuroimaging tech-

[1]others included in-vitro cultivation of neurons, ex-vivo hystophysiological analysis of in-vivo invasirely implantation of micro-arrays among others

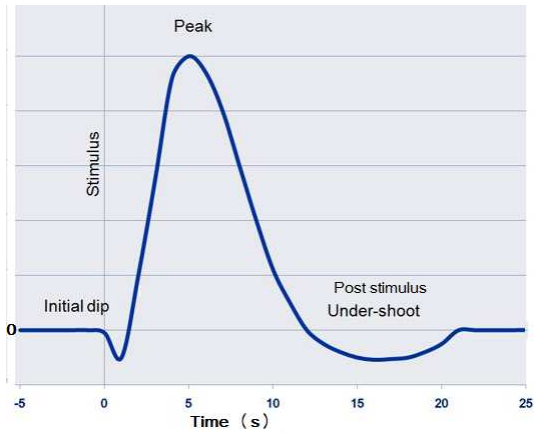


Figure 3.5: The classical signature of the BOLD hemodynamic response. The transient initial dip, reflecting an increase in oxygen consumption prior to the onset of increased blood flow and the peaks a few seconds after the onset of the stimulation (event stimulus applied at time $t = 0s$) can be appreciated the positive component of the HRF is very robust and ofen used to produce maps of functional activity. Figure reproduced from: $http://www.openwetware.org/wiki/Image:HRF.gif$

niques exploit different physical phenomena to reconstruct the direct neural activity or an indirect marker of it. Functional near-infrared spectroscopy (fNIRS) is a non-invasive neuroimaging technique Villringer *et al.* (1993) based on diffuse optics. The brain functional information is decoded through the interpretation of the variation in the optical properties of previously irradiated near-infrared (NIR) light Ferrari & Quaresima (2012). NIRS monitors the regional cerebral blood flow (rCBF) variations through the changes in absorption of the NIR light at wavelengths between $650 - 950nm$. Using fNIRS, brain activity is indirectly measured through the hemodynamic responses associated by the neurovascular coupling as explained in the previous section. Once the photons are radiated into the human head with a laser emisor (source), these cross through the different layers of the head (skin, skull, meninjes, grey and white matter, etc.) until absorbed or eventually exiting the head. Those photons having a higher probability of detection by the (paired) photodetectors are the ones at the tip of the banana shaped scattered beam as illustrated in Figure 3.6.

fNIRS measures optical density (OD) changes at two (or more) wavelengths, with the main changing chromophores responsible for those changes being the oxygenated and reduced hemoglobins which happens to be markers of brain hemodynamics in turn proxy of brain activity. The reconstruction of the concentration changes of the chromophores of interest is achieved using the modified Beer-Lambert Law Cope & Delpy (1988); Haeussinger *et al.* (2014); Sassaroli & Fantini (2004).

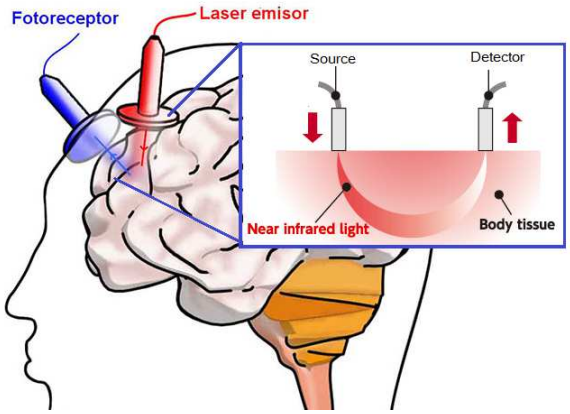


Figure 3.6: In fNIRS a photo-detector placed approx 2.5 cm away from the light source collects photons that are not fully absorbed and that have travelled along the banana shaped path between the source and detector. The interoptode distance regulates the depth at which the detector is more sensitive permitting probing regions 1-2 cm deep like the grey matter where most brain activity occurs. Figure modified from *http* : *//www.hamamatsu.com/jp/en/technology/lifephotonics/healthcare/trs/index.html* and *http* : *//www.saberesyciencias.com.mx/sitio/component/content/article/*10 − *portada/*522 − *la* − *neuroimagen* − *optica* − *soluciones* − *computacionales* − *a* − *un* − *problema* − *fisico*

# Chapter 4

# Related Work

This section first presents introductory examples of the use of differential manifolds for analysing a mechanical and a gravitational problem helping to illustrate how topology and manifolds are used for expressing the solutions of physical phenomena. Later, general work related to brain connectivity is presented. Finally the analysis of causality in the brain i.e. effective connectivity, are reviewed more closely.

## 4.1 Simple and double pendulum

Consider a simple pendulum confined to a plane as depicted in Figure 4.1. Every possible position of our system is completely determined by the magnitude of the angle $\phi$ in $[0, 2\pi]$. A single parameter is required to describe the magnitude of such angle. If the distances segment OA is normalized to length one[1], that corresponds to a position on the circumference that is usually denoted by $S^1$. The space of all possible states of our mechanical system is thus a manifold of one dimension, namely the circumference denoted by $S^1$.

Now consider the double pendulum in Figure 4.2. Every possible position is completely determined by the magnitude of the angles $\phi$ and $\psi$. The space of all possible states of the double pendulum is described by $S^1 \times S^1$ and this geographically corresponds to the coordinates of a torus. In physics, it is common to indicate that the mechanical system has two *degrees of freedom* and the space of possible solutions is sometimes referred to as the *configuration space*.

Points over the manifold may contain other information, such as the speed of movement of the particles. For example, suppose we have a particle that can move freely on a circle with an arbitrary velocity. The state of the system is described by two data items: the position of the point on the circle and the velocity at a given instant. Note that the direction of the movement is restricted i.e. the speed vector is irrelevant, not adding additional parameters. The manifold of system states (the configuration space)

[1]Normalization is only convenient, but note that it does not further introduces another parameter.

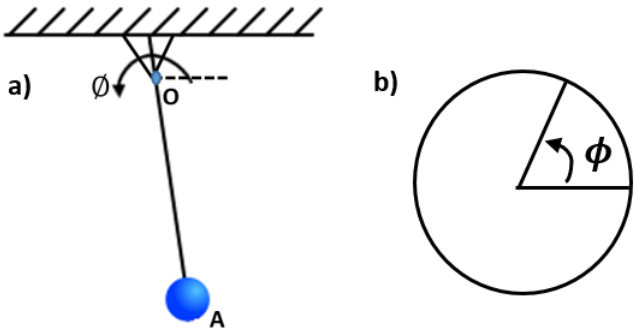


Figure 4.1: Simple Pendulum. The pendulum in *a*) consists of the segment $OA$; the point $O$ remains immobile while the segment $OA$ itself turns freely in a fixed plane at a fixed distance around $O$. The circumference in *b*) represents such set of possible locations in the plane and is denoted as $S^n = (x_1, \ldots, x_{n+1}) | x_1^2 + x_2^2 + \ldots + x_{n+1}^2 = 1$ is this particular example. Figure reproduced from Aleksandrov *et al.* (1999).

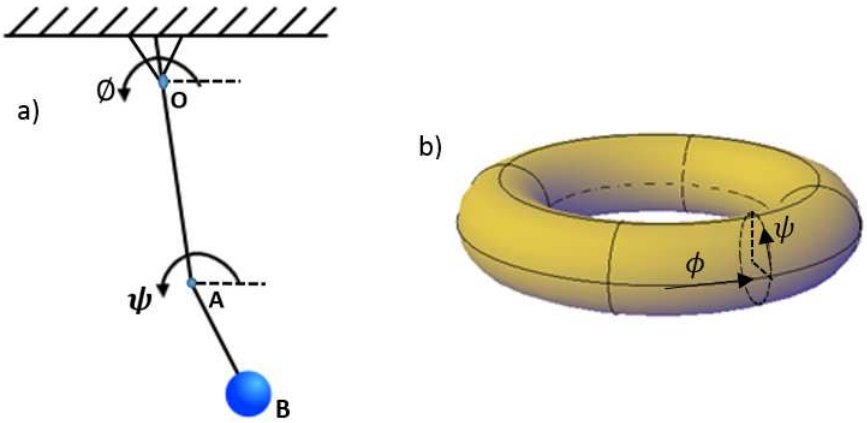


Figure 4.2: Double pendulum. The pendulum in a) consist of two segments $OA$ and $AB$ hinged together at $A$; the point $O$ remains immobile, the segment $OA$ turns freely in a fixed plan around $O$, and the segment $AB$ turns freely in the same plane around $A$. The torus in *b*) is the manifold denoted by $S^1 \times S^1$ and permits codification of all possible solutions to the system. Figure reproduced from Aleksandrov *et al.* (1999).

of this mechanical system is a cylinder; the product of a circle with a straight line. In general, the possible configuration space of a physical system inherently have a structure of a differentiable manifold of dimension $n$ Aleksandrov *et al.* (1999).

Under this fashion using a manifold-based modelling, solutions to the system correspond to specific locations in the manifold.

## 4.2 The four-dimensional space-time for relativity

Relativity explains gravity as an effect of the bending of spacetime in the vicinity of a massive object Collier (2012). A natural way to encode the spacetime are four dimensional manifolds in the Minkowski space Collier (2012), or perhaps more sophisticated 5 dimensional manifolds with a restricted smooth structure and an appropriate group of coordinate transformations Krym (2002). Usually, here locations in the manifold do not represent full solutions of the system but instead they only represent specific events. In a scenario analogous to the domain of this research, causal relations among events are soujht.

Under this fashion using a manifold-based modelling, solutions to the system correspond to world-lines or trips along the manifold. Note the contrast with the mechanical example above.

## 4.3 Manifold based analysis in neuroscience

The hypothesis expressed in this protocol; that the brain function abides the construct of manifold arises from previous work which have hinted that the brain function comply with the mathematical requirements of specific manifolds; continuous, differentiable, metric, etc. This section reviews this previous empirical modelling of neurophysiologic phenomena exploiting topological tools, which is further summarized in Table 4.1.

Table 4.1: Summary of manifold based analysis in neuroscience. Projection on the tangent space Euclidian (PTSE)

| Name | Distance function | Projection / Rendering | Manifold |
|---|---|---|---|
| Friston *et al.* (1996) | $1-$correlation | cMDS | Topological (not indicated) |
| Leff *et al.* (2007) | geodesic | cMDS (Isomap) | Riemannian |
| Ng *et al.* (2014) | Covariance | MWT,PT | Riemannian |
| Varoquaux *et al.* (2010) | Covariance | PTSE | Riemannian |
| Dodero *et al.* (2015a) | SD | LEM | Riemannian |
| Dodero *et al.* (2015b) | Graph Laplacian | LEM | Grassman |

In 1996, Friston *et al.* (1996) expressed the brain function in a $k$-dimensional space where points on the manifold represented local hemodynamics and used as distances between the points the correlation between events i.e. voxel timecourses. This projected the brain function to a hypersphere that Friston et al branded the *functional space*. Rendering of the manifold was achieved by classical multidimensional scaling (cMDS) Torgerson (1958) permitting exploration of the functional connectivity. This was the first example to the author's knowledge capitalizing on topological modelling to encode a neurophysiological phenomenon.

Much later, Leff *et al.* (2007) also studied brain activity utilizing manifolds. Distinctly from its predecessor Friston *et al.* (1996), this method exploited the geodesic of the manifold to explore the functional phenomenon. Isomap[2] was used Tenenbaum *et al.* (2000) for recovering the intrinsic dimensionality of the non-linear structure of the neuroimaging data which permitted discrimination of expertise related differences in brain's response to a surgical knot-tying task. More recently, the geometric properties of the geodesic distance over symmetric positive definite (SPD) matrices forming a Riemannian manifold were exploited again to study functional connectivity. In Ng *et al.* (2014, 2015), the authors attempted to retrieve functional connectivity patterns before and after a certain linguistic intervention in a longitudinal study. To achieve their goal, they expressed the functional connectivity as features of the covariance matrices among the neuroimage scans. In these papers, the covariance matrices live on the space of the positive semidefinite cone Varoquaux *et al.* (2010). They treated the positive semidefinite cone as a Riemannian manifold and projected the covariance estimates onto a common tangent space to this manifold. Each point on the manifold surface corresponded to one subject, while the projection of the tangent space to a Euclidean space is a diffeomorphism generated by the matrix whitening transport (MWT) and parallel transport (PT) Thorpe (1994). This is a more sophisticated exploitation of the expressive power of manifold-based modelling, but causal relations were not sought.

Finally, Dodero *et al.* (2015b) recently took advantage of manifold embedding techniques to kernelize a classification task. In particular, they used kernel Support Vector Machine (SVN) Shawe-Taylor & Cristianini (2004) applied to connectivity matrices for their classification task. In both approaches, points on the manifold are connectivity matrices i.e. full system solutions, and the manifold were explored (rendered) with a diffeomorphism dictated by the Log-Euclidean metric (LEM) Arsigny *et al.* (2005) where distances were given by the Stein divergence (SD) Sra (2011) for Dodero *et al.* (2015b) kernel based approach using projection metric on a Grassman Manifold[3] respectively, both computed using regularized Laplacians.

Despite these modelling attempts, none of the previous work actually produced any evidence whatsoever that the brain function behaves as a manifold. This, in all cases, was simply assumed.

## 4.4 Modelling of brain's effective connectivity

The analysis of effective connectivity has not yet been attempted by topological means. Commonly, coherence based, probabilistic and statistical approaches dominate the landscape. This section and the companion Table 4.2 summarize these.

[2]Isomap is actually the cascade of the calculation of the geodesic and the subsequent projection with classical multidimensional scale.

[3]Given a space $\mathbb{R}^n$, the Grassman manifold is the set of linear subspaces of dimension $k$, $0 < k \leq n$ does not lie on the Euclidean space but on the Riemannian manifold.

Table 4.2: Summary of popular modelling approaches for effective connectivity.

| Name | Approach | Context | Temporal Precedence | Neural Interactions |
|---|---|---|---|---|
| DCM (Friston *et al.*, 2003) | Differential equations | X | X | Dynamic |
| SEM Büchel & Friston (1997) | Differential equations | X | | Linear |
| DTFKaminski & Blinowska (1991) | Coherence | | X | Linear |
| PDC Baccalá & Sameshima (2001) | Coherence | X | X | Linear |
| Proposal | Topological | X | X | Dynamic |

Structural equation modeling (SEM) Büchel & Friston (1997); Biddle & Marlin (1987) is a multivariate, hypothesis-driven technique that is based on structural models (i.e. differential equations) representing a hypothesis about the causal relations among several variables. For example, variables are the measured blood oxygen level-dependent (BOLD), brain regions and the hypothetical causal relations are based on anatomically plausible connections between the regions. Under SEM the causal relationships are not inferred from the data but assumed a priori, and only confirmatory analysis is carried out. Despite being oblivious to temporal information, SEM remains a popular approach for the analysis of effective connectivity since it was first introduced for this use by McIntosh & Gonzalez Lima (1994).

Coherence based methods are routinely used to retrieve the causal graph in neuroimages. The directed transfer function (DTF) Kaminski & Blinowska (1991) technique is a full multivariate spectral measure used to determine directional influences between any given pair of signals in a multivariate data set. DTF is based on the spectral Granger causality Kamiński *et al.* (2001), according to which an observed time series $s_1(t)$ causes another time series $s_2(t)$ if the knowledge of $s_1(t)$'s past significantly improves prediction of $s_2(t)$. The relationship between these two time series is not reciprocal, so it is possible to determine the direction of information flow between the time series. A closely related coherence based approach, also inspired in Granger causality is Partial directed coherence (PDC) Baccalá & Sameshima (2001) which differs from DTF in its ability to capture the transitive relations; DTF see transitive relations but cannot appreciate the intermediate path whilst PDC only see pairwise relations but cannot see transitive relations.

Dynamic Causal Modeling (DCM) is an *ad-hoc* modelling approach that has become the *de facto* standard for the analysis of brain effective connectivity Friston (2011). DCM (Friston *et al.*, 2003) is a Bayesian framework for estimating experimentally induced changes in effective connectivity, once the causal model has been translated from neuronal activity to predicted data, it can be compared to the observed data to estimated the unknown parameters of the model, including the synaptic couplings. Like SEM, DCM is a hypothesis-based confirmatory approach, the latter being carried out using a Bayesian framework. DCM is distinguished from alternative approaches not just by accommodating the nonlinear and dynamic aspects of neuronal interactions, but by

framing the estimation problem in terms of perturbations that accommodate experimentally designed inputs.

## 4.5 Transformations

### 4.5.1 Neural response models

Spike generation with the dynamics of the Hodgkin-Huxley model is a mathematical model of current flow through ion-selective channels in neural membrane Beeman (2014) which describes how action potentials in neurons are initiated and propagated to another and describes the time behavior of the intracellular membrane potential and the currents through potassium (K) and sodium (Na) channels with simple first-order ordinary differential equations Gerstner & Kistler (2002).

Heeger's Poisson Model of Spike Generation Heeger (2002) proposes that in the cortex, the timing of successive action potentials is highly irregular. Then, the irregular interspike interval reflects a random process and implies that an instantaneous estimate of the spike rate can be obtained by averaging the pooled responses of many individual neurons. The spike train would be completely described as a particular kind of Poisson process.

### 4.5.2 Hemodynamic response models

The hemodynamic response refers to the changes in blood irrigation locally to an active brain region and it is mediated by the neurovascular coupling. This response alters the flow (CBF) and volume (CBV) of blood subsequent to changes in the metabolic rate of oxygen (CMRO2) following neural firing, in turn altering the baseline balance of oxygenated and reduced haemoglobin. This hemodynamic response is critical for those neuroimaging modalities that capitalize on these indirect hemodynamic markers of brain activity. The different models expressing the relation between the neural activity and these hemodynamic changes are referred to as hemodynamic response functions (HRF), but their specific form, not only depends on the neurovascular process itself but also on the neuroimaging modality observing it. Hemoglobin (Hb) is diamagnetic when oxygenated and paramagnetic when reduced. In functional magnetic resonance imaging (fMRI), the presence of deoxyhemoglobin alters the local magnetic susceptibility. The signature of such alteration is known as the blood oxygen level dependent (BOLD) signal, and this effect is a valuable tool for mapping brain activation. In Buxton *et al.* (2004) the mathematical relation between the hemodynamic parameters CBF, CBV and CMRO2 and the fMRI observable BOLD signal is established resulting in a biologically elaborated version of the HRF for fMRI. A much simpler[4] statistical description of the BOLD signature, is that comprised the sum of two gamma functions Friston *et al.* (1998),

[4]And popular due to the success of the statistical parametric mapping analysis of brain activity.

but this one lacks the biological foundations. In diffuse optical imaging, the modelling of the hemodynamic response accounts for temporal changes observable in the remitted spectra due to those changes in tissue absorption in turn attributable to changes in haemoglobin concentrations (of both, HbO2 and HbR) taking advantage of the different absorption coefficients exhibited by the two haemoglobin species Huppert *et al.* (2006), moving from the univariate domain of BOLD-fMRI to the multivariate domain of fNIRS. Literature also offers different models of the optical HRF. Zhang et al Zhang *et al.* (2005) described the optical HRF in terms of a basis function expansion in a joint spatio-temporal reconstruction of the diffuse optical imaging. Diamond et al Diamond *et al.* (2009) built a sophisticated biologically plausible model of the optical HRF taking into account some of the systemics including heart rate, arterial and venous compliance. A summary of these is presented in Table 4.3. Regardless of the neuroimaging modality, the objective of hemodynamic response models is to have a function that describes the expected recognizable local signature recorded by the neuroimage when a certain neural population fires. Collaterally, it further helps to separate out the background systemics in neuroimaging data.

Table 4.3: Summary of popular modelling approaches for hemodyanmic response.

| **Name** | **Type** | **Approach** |
|---|---|---|
| Buxton *et al.* (2004) | BOLD | Differential equations |
| Friston *et al.* (1998) | BOLD | Statistical |
| Zhang *et al.* (2005) | Optical | Function expansion |
| (Diamond *et al.*, 2006) | Optical | Differential equations |

### 4.5.3 Image reconstruction models

The formation of an image is the consequence of some form of radiation interacting with matter, and in the case of diffuse optical imaging, and its neural version fNIRS, the interaction of electromagnetic radiation with one or more internal optical characteristics of the tissue Arridge & Schweiger (1997). As shares of the radiation abandon the tissue and reaches the photodetectors, this energy is transduced most often into electrical recordings. The necessary companion to the image formation process is therefore the image reconstruction, translating the sensor output into the histophysiological magnitudes of interest. In the case of fNIRS, the changes in hemoglobin concentrations. The transport of radiation in tissue ruling the image formation is dictated by the Radiative Transport Equation (RTE) Branco (2007) ; a balance equation that has into consideration the changes in energy flow, in time and in an infinitesimal volume, due to gains of incoming energy by a light source or by scattered photons and energy losses due to photons leaving the volume or absorbed energy. The analytical complexity of the RTE

means that exact solutions are limited in practice to extremely simple geometries Branco (2007). Hence, a number of approximations, numerical like diffusion theory or Kubelka-Munk, and stochastic like Monte Carlo or Random Walk have been developed. In fNIRS, arguably the most successful of these approximations to model image formation is the Modified Beer-Lambert Law (MBLL) Delpy *et al.* (1988). Its predecessor, the Beer Lambert law describes the loss of light intensity as radiation travels through a non-scattering medium i.e. attenuation is attributable only to absorption. Since biological tissue is highly scattering, the MBLL incorporates a factor that accounts for tissue geometry and light attenuation due to scattering so that scattering can be considered constant, and then compensates this assumption by adding the Differential Path-length Factor (DPF) that accounts for the increased distance that the light travels Scholkmann *et al.* (2014). Having chosen a forward model of radiation transport to express the image formation, the model has to be inverted so to recover tissue parameters from the space of sensor outputs by a companion image reconstruction approach. In the case of MBLL, the reconstruction i.e. the inversion method, is simply the system of equations derived resulting from clearing the concentration of the chromophores of interest. For $n$ chromophores, the equation should be evaluated at $n$ different wavelengths. Common options for image reconstruction approaches include linear methods such as the perturbation method based on inverting the Jacobian of the system, and non-linear methods like gradient-based reconstruction and Newton-like methods Herrera-Vega & Orihuela-Espina (2015). An alternative strategy is the computation of the so called colouration map. The reconstruction based on the colouration map re-expresses the inverse problem as an optimization problem whereby the vector of recovered parameters is the one whose precomputed associated remitted spectra best fits the observed spectra.

## 4.6 Chapter summary

The opening sections of the chapter offer a wide range of manifold based modelling possibilities whereby locations in the manifold in each case represent a different entity. For those closer to the domain at hand, regardless of the opted methodology, none of these previous works produced any evidence that the brain behaviour was confined to the manifold where solutions were expressed; this was simply assumed as highlighted. However, the insightful reader would quickly appreciate from these works how the fluctuations of the underlying behaviour from one point to a neighbour point within the assumed manifold were smooth, suggesting a continuous and differentiable behaviour of the system, both properties to be expected in a locally flat object. Computationally this leaves much to explore as the properties of the input space is fully unknown.

Also, although in external domains e.g. relativity, causality has been a driving force to exploit manifolds, this still seems underexplored in neuroscience. The computational implications of imposing causally inspired deformations to the manifold or instead opting for exploiting the causal structure naturally present in the manifold with negative signa-

ture remain unknown. It is anticipated that it is actually the specific choice of possible alternatives in the chain of transformations that are likely to dictate the computational consequences.

The manifolds of Riemann spaces exist in a positive symbol that are more intuitive and which is easier to operate. While Lorentz manifold incorporate inherently causality interpretation is not trivial. Modeling on Riemannian structures could be a sufficiently good approximation given certain conditions that are to be explored in this thesis.

# Chapter 5

# Research proposal

In this chapter the methodology intended for the development of this research is presented. Also, the experimental design for the collection of in-vivo data, schedule (Figure 5.1) and publications plan are further described.

## 5.1 Methodology

The following describes the methodological steps intended for the development of the proposed research:

1. **Familiarization with computational neuroscience**

   Familiarization with the necessary background knowledge on topology, vector calculus, neurophysiology and neuroimaging as well as computational modelling in neuroscience (i.e. computational neuroscience). Collaterally advances will be made towards exploting different representation on neurological signals as a cloud of points in space.

2. **Transformations among spaces**

   Selection of a set of appropriate kernels (transformations among spaces) for the stimulus train, the neural firing, the hemodynamic response and the optical imaging formation and reconstruction. Elaboration of these transformations is not the aim of the thesis, so suitable ones will be taken from literature. The task is not so much the development of new mappings but the characterization of the topological properties of the kernels chosen, i.e. the deformation they impose on the manifold.

3. **Generation of forward synthetic scenarios for verification purposes**

   Synthetic scenarios will be generated. These scenarios will have latent causal relations between variables. The proposed models in subsequent steps of this methodology will be verified against this dataset for which the ground truth is known.

One possible approach for the generation of the synthetic scenarios is using differential equations as in Kamiński *et al.* (2001). At least, the following scenarios are intended;

- Two dynamic variables $(X, Y)$
  - There are no relationship between the variables, $X$ and $Y$
  - One variable causes the other variable, $X \rightarrow Y$
- Tree dynamic variables $(X, Y, Z)$
  - The relationship between variables are: $X \rightarrow Y \rightarrow Z$
  - The relationship between variables is $X \rightarrow Z$; there is not relationship with variable $Y$.
  - There is no relationship between any of the variables, $X, Y, Z$

4. **Semantics of topological loci**

   Establish the domain specific meaning of the points in the topological space. This results from the concatenation of the above kernels (composition of functions) in order attach specific domain (neurophysiological) meaning to locations in the manifold which can express the relationships between them. A dictionary of concepts between neuroscience and topology has to be establish, in a manner analogous to that in Chamizo (2015) for a mechanical example. Further, initial decisions over the meaning of the solutions in the manifold-based modelling approach will be taken. Finally, the first research question will be answered here; a specific manifold yet to be chosen depending on the properties determined in the previous tasks encoding some domain phenomena e.g. segregational, will be built and rendered.

5. **Encoding of causality by means of an imposition of a causally inspired distance function**

   First, the inability of the ambient induced distance function e.g. Euclidean, to express the construct of interest will be shown. Then a new distance function shall be incorporated to the topological space of the Riemann manifold that allow migrating from functional to effective features of brain activity to be expressed and analyzing the deformation suffered by the manifold when the new distance is imposed. The objective of this task is to obtain a model of the functional connectivity based on the Riemann manifold. Again, the final selection of the manifold might not be Riemann's but this preliminary choice is made on the current empirical evidence of previous works. It remains unclear whether existing coherence based distance functions such as direct transfer function Kaminski & Blinowska (1991) or partial directed coherence Baccalá & Sameshima (2001), or perhaps more sophisticated theoretical information based functions as for instance transfer entropy Katura *et al.* (2006) may actually have face validity or a new distance function will

have to be designed. Verification of the resulting topological modelling approach will be carried out over synthetically generated data. This task intends to answer the second research question.

6. **Encoding of causality by means of extension to negative signature spaces**

   Explore the extension of the previous modelling approach to negative signature spaces. Harness a causal topological space such as Lorentz manifold that allow effective features of brain activity to be expressed and again analyzing the deformation suffered by the manifold when the new structure is imposed. The objective is to obtain a modelling approach of the effective activity that inherently incorporates a causal structure. Verification of the resulting topological modelling will be carried out over synthetically generated data. This task aims to answer the last research question.

7. **Validation of the models**

   The final step is dedicated to the confirmation of the main computational and neurophysiological hypothesis presented in the introductory chapter. The ability of the two modelling approaches for encoding effective relations across a chain of transformations; (i) positive signature space plus causally inspired distance function, and (ii) inherently causal manifold, to make predictions that match experimental observations will be put to test. The description of the experimental design to acquire real observations is further described below. Also, comparison of the proposed models with other solutions existing in literature such as Structural Equation Modelling as well as including the gold standard Dynamic Causal Modelling will be made. Nomological validity will be sought.

## 5.2 Experimental design

A domain specific experiment will be carried out. A cohort of participants will be recruited. The participants will be stimulated with a certain, either cognitive or motor task, following the classical block design paradigm. Since the ground-truth in non-invasive neuroimaging is unavailable, critically the task choice will be made such that the stimulus given evokes a well-known neural circuit. Optical neuroimaging data will be collected from the cohort. Images will be reconstructed using the modified Beer-Lambert law. Data will be processed according to typical fNIRS processing for instrumental and systemic noise attenuation Orihuela-Espina *et al.* (2010). Brain activity will be confirmed using alternative classical statistical task minus baseline analysis Tak & Ye (2014) and/or statistical parametric mapping (SPM) Friston (1994) to partially confirm that the assumed recruited circuit is active during the stimulation. Finally, the neuroimaging dataset will be analysed for effective connectivity with both the proposed approaches and the existing alternatives. Concurrent validity will be established by similarity of

the recovered solution with respect to the gold standard. Nomological validity will be discussed against literature.

Part of this experiment will be carried out during a research secondment in University College London (approximate dates; from March 2016 to July 2016) at the Biomedical Optical Research Laboratory under the supervision of Dr. Ilias Tachtsidis. It is intended that the experiment design will be delineated prior to the secondment, and final details as well as data collection to take place in while in London.

## 5.3 Schedule

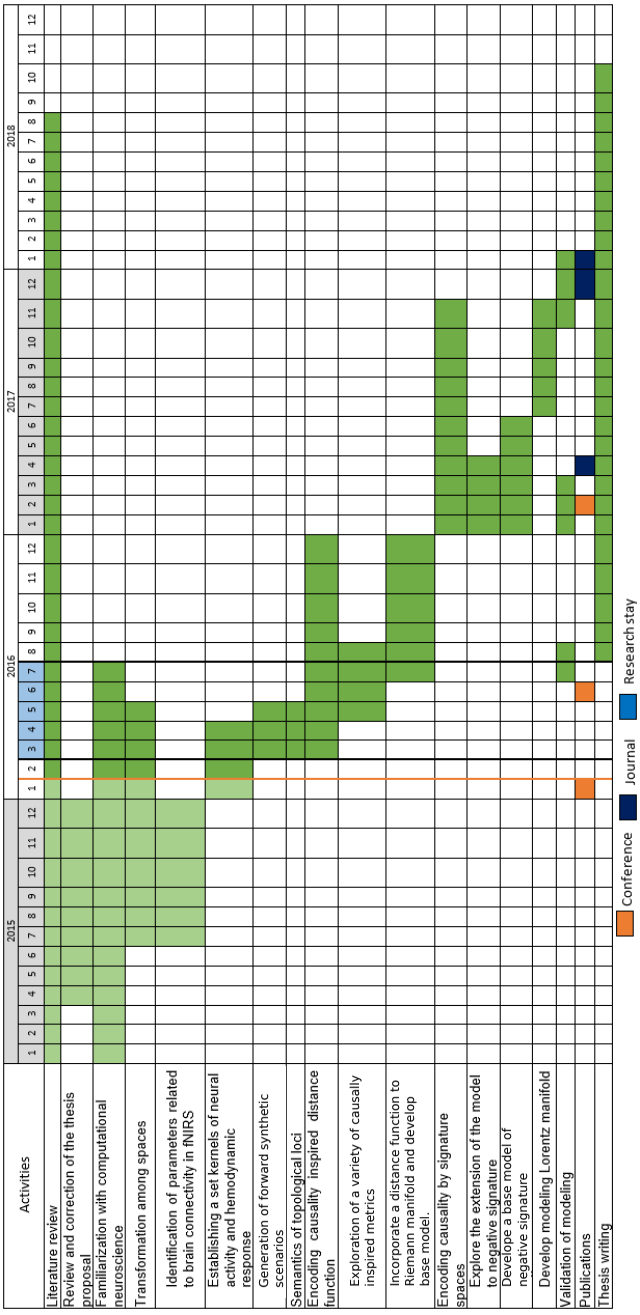


Figure 5.1: Task scheduling and current progress.

## 5.4 Publications plan

The intended publications and targets are indicated below

1. **Conference paper (abstract only):**
    - Target: 2nd International Conference on Mathematical NeuroScience (ICMNS)
    - Aim: Position paper expressing the main hypothesis of this research
    - Associated research question: research question 1 and main hypothesis.
    - Expected results: Preliminary advances presented in chapter 5 of this protocol.
    - Estimated submission time: Submitted. Deadline 15th January 2016
2. **Conference paper (full length):**
    - Target: 31st Neural Information Processing Systems (NIPS) 2017. (Biennial) Top conference in computational neuroscience, neuroinformatics and neurocomputing.
    - Aim: Modelling of segregational function and establishment of semantics of topological loci
    - Associated research question: research question 1.
    - Expected results: A preliminary manifold based model of a segregational phenomenon and the characterization of the computational properties of the input space.
    - Estimated submission time: June 2016
3. **Conference paper (abstract only):**
    - Target: Functional near-infrared spectroscopy (fNIRS). Only world-wide conference exclusively dedicated to fNIRS neuroimaging.
    - Aim: Gathering of domain specific experimental data. Secondary; Familiarization with experimental techniques in neuroimaging experiments.
    - Associated research question: All.
    - Expected results: Advances made during the research secondment on UCL. Prelimary analysis of brain activity on the collected dataset
    - Estimated submission time: June 2016
4. **Journal paper:**
    - Target: Journal of Computational Neuroscience (IF: 1.73)

- Aim: Establishment of the foundations of topological modelling of brain connectivity
- Associated research question: research questions 2 and 3.
- Expected results: Characterization of the deformations suffered by the manifold as it traverses different spaces as a result of transformations.
- Estimated submission time: March 2017

5. **Journal paper .**

- Target: Neuroimage (IF: 6.35)
- Aim: Proposition of two computational modelling approaches for the retrieval of brain's effective connectivity.
- Associated research question: research questions 2 and 3.
- Expected results: Validation of proposed models.
- Estimated submission time: End of 2017

# Chapter 6

# Preliminary progress

This last chapter presents some of the preliminary ideas and advances made during the first year.

## 6.1 Transformations among spaces and forward model

As suggested in the problem statement, it is possible to model the flow of information from the neural firing and connectivity to the eventual observation of its hemodynamic consequences in the neuroimage as a composition of functions or transformations of the information across spaces. Although the chain of transformations described in chapters 1.3 and 4.5 make no explicit mention of an external stimulus, the brain is capable of initiating its own activity, and therefore it is customary to add an additional transformation to consider such external stimulus. In fact, the addition of other information such as the incorporation of systemic effects, the sensing geometry, etc could have been equally considered. They will however, by now be excluded from this research for the sake of simplicity though. This chain of transformations is depicted in Figure 6.1.

Figure 6.2 shows an exemplary transformation of the information from a stimulus train to an expected hemodynamic response of a single neural population assumed to fire with the stimulus. The choice of the kernels for this specific example is irrelevant as the only aim is to illustrate the transformations themselves. However, for the real modelling the selection of these kernels has an impact on the manifold construction and deformation. The second of the research tasks indicated in the methodology is in fact the selection of a set of appropriate kernels (transformations among spaces) for the stimulus train, the neural firing, the hemodynamic response and the optical imaging formation and reconstruction. Literature already offers a number of choices for the different kernels, and current efforts are made to select the ones that will be used for this research, and to characterize the topological properties of the kernels chosen. Although still using the naive kernels in Figure 6.2, the modelling of a small group of 4 neural populations has already been simulated with two of them not responding to the stimulus.

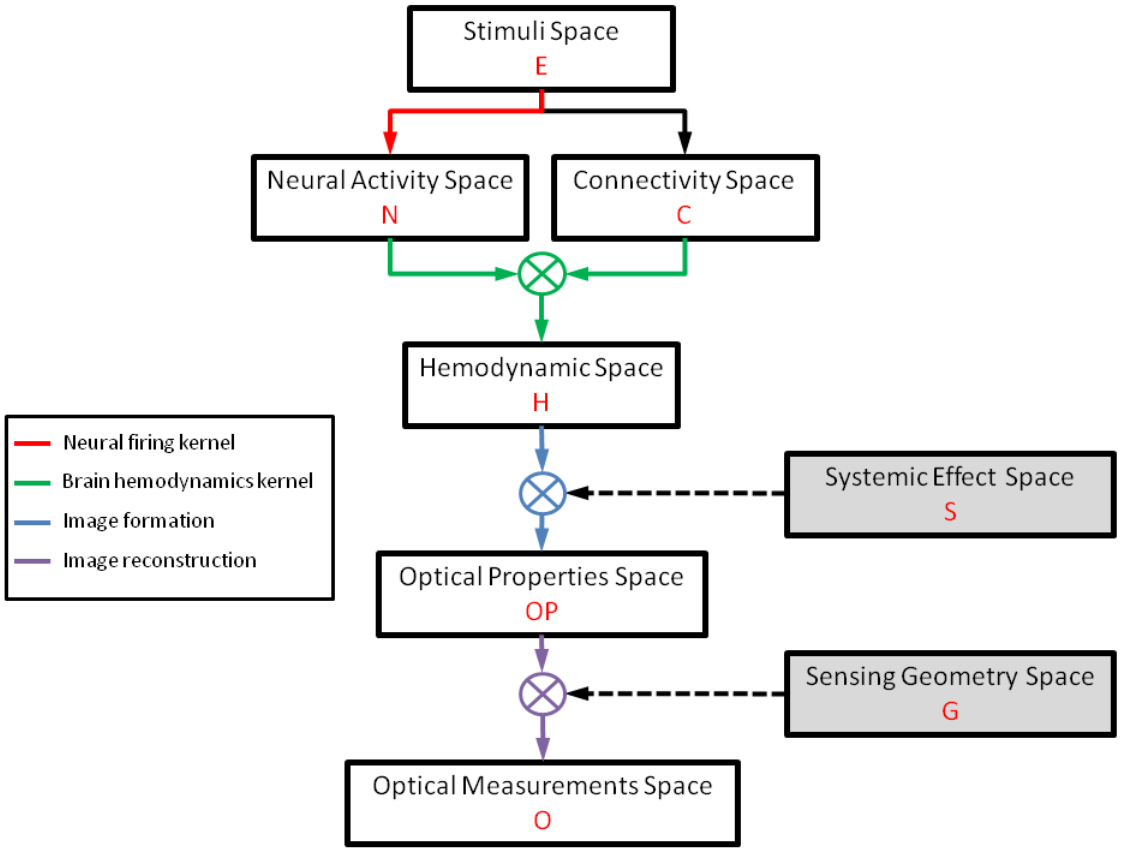


Figure 6.1: The journey of the information. The chain of transformations among spaces is depicted. The incorporation of certain stages and additional information is customary and reflect different degree of the model fidelity to the physical process. Here the spaces and kernels that will not be considered in this research are exemplified with grey shaded and dashed lines respectively.

## 6.2 Representation of temporal signals as points in a space

Let $s(t)$ be a signal or time series such that $s(t) = \{s_k | k = 1, ...K\}$ where $s_k$ is the amplitude value of the signal in k-th instant of time. If each moment of time e.g. sample, is considered as a dimension in a certain space, and the amplitude of the signal at that sample the coordinate value along that dimension, the signal $s(t)$ becomes a point of this space, as exemplified in Figure 6.3. The generated space has of course $K$ dimensions.

A neuroimage can be seen as a set of signals in time; one signal being the values recorded at each channel, and thus can be represented as

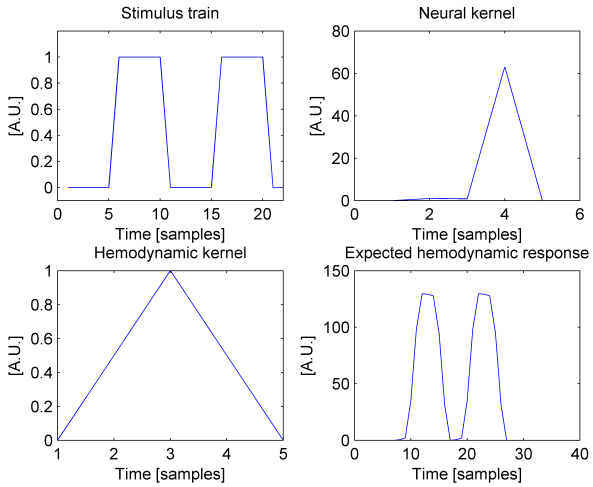


Figure 6.2: Expected hemodynamic response. The transformation from a stimulus train to an expected hemodynamic response of a single neural population assumed to fire with the stimulus. The choice of kernels in this example is naive and arbitrary. In this particular example the transformations have been achieved by convolution.

- a set of points or cloud in the $K$-dimensional space, where each point represents a descriptive behaviour at a location (i.e channel).
- As a single point in a $K \times M$-dimensional space with $M$ being the number of channels.
- Even perhaps by block splitting, the neuroimage can become a cloud of points in a $K_B$ dimensional space with $K_B$ the lenght of the block.

This permits thinking of a neuroimagen as either a single point or a distribution of points in a space. The distance function has therefore to be designed according to our needs to either estimate similarities among specific points or among full distribution of points, in turn permitting different types of analysis. For instance, when viewed as cloud of points it maybe suitable to compare neuroimages with a distance function comparing distributions, or perhaps a point-to-point distance function may reveal connective patterns. Moreover, arbitrary selection of subsets of points enables analysis by regions of interest. Or alternatively, when viewed as single points, a classic point-to-point distance function may permit elaboration of longitudinal changes in brain activity, or a distributional distance function can expose differences among sub-cohorts or groups of subjects. It is actually the combination of the representation and the imposed distance function i.e. the manifold!, which dictates what is a solution to the system and how it is represented, and consequently what is the phenomenon being exposed.

The following considerations have to be made:

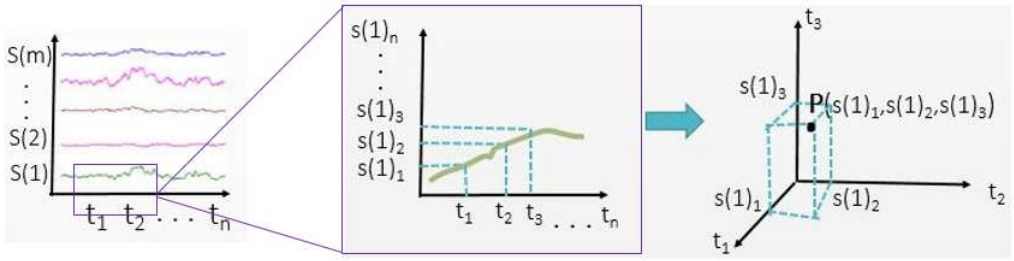


Figure 6.3: A signal $S(t)$ as a point in a k-dimensional space

- Each point in space is a signal $s(t)$ (or a concatenation of them e.g. a neuroimage)

- When the signal is represented as a point in a space it loses its temporal relationship. That is, the dimensions have no specific sequence or order unless it is externally imposed.

- If the temporary structure is to be recovered, then the Euclidean distance in this space has to be abandoned as an expression of the similarity of the signals (see Section 6.3), or equivalently as a form of closeness between points. It is therefore necessary to establish alternative distance functions along the manifold to express the construct of interest.

- This representation has to be univocal. Two signals with the same values at different time points have to project to distinct points to ensure a 1 to 1 relation.

- A point can be expressed as a function: $T \to S : \mathbb{R}^n \to \mathbb{R}$ or can be thought of as multidimensional signals $T \to S : \mathbb{R}^n \to \mathbb{R}^m$.

- Optical neuroimaging involves multivariate data at each recording ($\langle \mathrm{HBO}_2, \mathrm{HHe} \rangle$). Either the ambient space in unfolded to accommodate the univariate components individually or modelling has to be made over complex $\mathbb{C}$ spaces.

Note how a cloud of points in space can determine a graph; simply having a given $\epsilon$ that reflects the minimum radius at which should be another point to be considered that it is connected. This is a particularly useful observation since the connectivity network forms a graph.

As was mentioned, the Euclidean metric in this space does not have a clear meaning with respect to the notion of proximity among signals. It is necessary to build a space i.e. imposing a distance function where the location of the points reflects the same similarity. This is equivalent to understand the point cloud as a manifold.

## 6.3 Inadequacy of the Euclidean distance

Let $s(k, m)$ a neuroimage with a sequence of dynamic signals recorded at a number of head surface location (channels) i.e. $s(k, m) = s_{k,m}|k = 1, \dots N, m = 1, \dots M$ where $s_{k,m}$ is the amplitude of the signal in the $k$-th instant of time at the $m$-th channel. Often the neuroimage is the result of a recording expanding several stimulation trials or blocks. Two common analysis in neuroimaging, both of which have been used in manifold based neuroimaging analysis, work with either the full timecourse of the channel behaviour e.g. Friston *et al.* (1996), or splitting the neuroimage in small chunks corresponding to blocks. It is further customary to apply block averaging to increase signal to noise ratio (at the cost of statistical power) or to resample blocks to account for self-pace differences in trial execution. Regardless, each individual timecourse chunk that is to be passed to further analysis can be considered as datum in a space; the so called *Experiment Space*. The full dataset output by a neuroimaging experiment forms a cloud of points in this Experiment Space.

In going from a time series representation to a point representation in the Experiment Space, the temporal information is lost unless an ordering of the space dimensions is enforced. Regardless of whether such ordering is imposed, this section intends to illustrate that the ambient Euclidean distance among points in the space is not necessarily a good metric of signal similarity which has direct implications for the construct at hand. Indeed, signal similarity i.e. temporal correlation, is the support for functional connectivity.

Consider the concept of signal similarity between two points as the metric i.e. the metric encodes whether two points in the space are close or far. For example supposed an simple case where the neurosignal are composed of only six channels (for no particular reason) and that the neuroimagen is only scanned at two samples (for the sake of visualization) i.e. six signals with two time samples each. Since we only have two samples, and each sample translate into a single dimension in the experiment space, this space is a two dimensional space, where component one is perhaps the first time sample and component two is the second time sample. The mapping of the channel signals in the Neuroimage space into the Experiment Space is represented in Figure 6.4.

Consider the following fictitious Neuroimage Space: $s_1(t) = 2, 2, s_2(t) = 7, 7, s_3(t) = 2, 3, s_4(t) = 3, 4, s_5(t) = 3, 4, s_6(t) = 4, 6, s_7(t) = 4, 6, s_6(t) = 1, 0$. The points $s_1(t)$ and $s_2(t)$ will present a perfect correlation, and therefore the correlation coefficient between these two signals will be 1. Analogously, the correlation coefficient of points $s_3(t), s_4(t)$ and $s_5(t)$ will also be 1. This is so because the correlation function is independent of the scale. Hence, although $s_5(t)$ rises faster, the trend around its mean is the same as in the other two signals. Finally, signal $s_6(t)$ behaves completely opposite to these three $s_3(t)$, $s_4(t)$ and $s_5(t)$ and therefore it will have a correlation coefficient of $-1$ against each of them. $s_1(t)$ and $s_3(t)$ lay close together in the Experiment space (in the Euclidean sense), which is undesired.

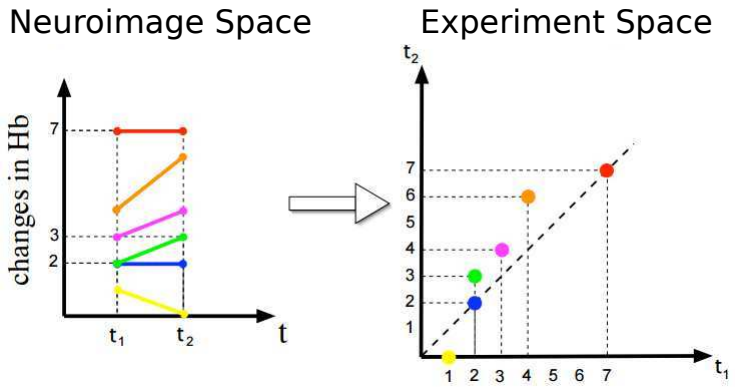


Figure 6.4: An example of the transformation from the time series in the Neuroimage Space to the point representation in the Experiment Space.

The more different your amplitude, the more distant you will be in this space. Furthermore, for points with the same difference in amplitude they will be at the same distance, with the correlation sign somehow reflecting whether you move upwards or downwards. This simple example illustrates why the ambient Euclidean distance is not a good choice to express connectivity related constructs, hence the importance of choosing the metric and semantics of the space of connectivity to interpret the data.

## 6.4 Example

The rationale of the example is as follows. First, transform the timecourse observed at every channel to an arbitrary point in a certain space. Second, impose a metric i.e. a metric tensor (perhaps even as naive as reusing the Euclidean ambient distance) that in its essence matches the construct of the brain phenomenon being modelled. In this example, the brain phenomenon is functional connectivity, and thus the metric has to encode signal similarity. Although, these two previous steps are themselves the modelling i.e. the manifold representing the brain phenomenon is already defined by the metric tensor, they are often accompanied by a third and final step to facilitate model interpretation. Thus, finally, the manifold is often projected to or embedded into a low dimensional Euclidean space for visualization. Suppose that we have acquired a set of neuroimages and perhaps that we are interested in retrieving the functional connectivity encoded in one of them. Since functional connectivity is about different brain regions exhibiting associative correlational activity pattern, we are interested in building a manifold where co-active regions manifest themselves as close loci in the surface. For the sake of simplicity, in this example it is assumed that the information recorded at every channel is univariate -we briefly hint later that this is not a constraint to this modelling approach-. Also, again for simplicity, it will be assumed that each

channel is a good proxy of one brain region of interest and that there is no overlap among observed brain regions. The methodology is as follows:

- Projection to ambient space: Abstract each channel behavior as a point in a certain ambient space. This is equal to transform each signal of the neuroimage (channels) into a point in an arbitrary space that in this example we will call Experiment or Experimental Space. If the reader is familiar with machine learning technique it will quickly associate this with the raw feature space.

- Definition of the manifold: In the Experimental Space, order the points. Briefly, an order is a particular indexing of the elements of a set and in topology this equates to defining a distance function among the elements of the topology. The distance function has therefore to be designed according to our needs permitting either estimating similarities among specific points or among full distributions of points in turn permitting different types of analysis. As a consequence of point 2, a manifold is defined. The manifold has been built in such way that channels exhibiting similar temporal behavior are projected to close locations in the manifold surface.

- Definition of the solution to the brain phenomenon (e.g. Construction of the graph of functional connectivity) Now we need establishing the (functional) connectivity between points as a certain characteristic of the previously built manifold. Note how a cloud of points in space can determine a graph; simply having a given $\epsilon$ that reflects the minimum radius at which should be another point to be considered that it is connected (or perhaps assuming a fix number of neighbor points). This is a particularly useful observation since the connectivity network is simply the result of the epsilonadjacency among observed points e.g. channel timecourses in this case.

- Renderization: Finally, a more familiar characterization of the result is provided by rendering the connectivity network as a graph. The graph expresses the (functional) connectivity of the cerebral regions encoded in the original neuroimage.

- Renderization: Finally, a more familiar characterization of the result is provided by rendering the connectivity network as a graph. The graph expresses the (functional) connectivity of the cerebral regions encoded in the original neuroimage.

### 6.4.1 Generation of synthetic data

The generated synthetic dataset consists of a small group of 4 neural populations with the four responding to a given stimulus but affected by a certain amount of noise. This noise might (or might not depending on the choice of the epsilon) prevent the observation of the coactivity among the four regions. The expected observed haemodynamic response

at the different channels was calculated from the convolution of the stimulus train, neural firing and haemodynamic kernels see 6.5. Assuming an ideal imaging process (i.e. the image space faithfully represents the hemodynamic space) and ignoring the processing; the observed image value $O(t)$ at a certain channel $C$, $OC(t)$ when the brain is presented with a given stimulation $S(t)$ that excites the neuronal population interrogated by the stimulus is given by:

$$OC(t) = S(t) \otimes NFK(t) \otimes K(t)$$

where $NFK(t)$ is the neural firing kernel for an excited neuronal population and $HK(t)$ is the haemodynamic kernel and ï$f_{\text{„}}$ represents the convolution. The choice of kernels with regards to shape, timing and amplitude of responses used in this example is intentionally naive and arbitrary. The only purpose is exemplification. Finally, this ideal response is contaminated with white noise (5% or less of signal range) to get variability in the signals. $OC'(t) = OC(t) + whitenoise(t)$

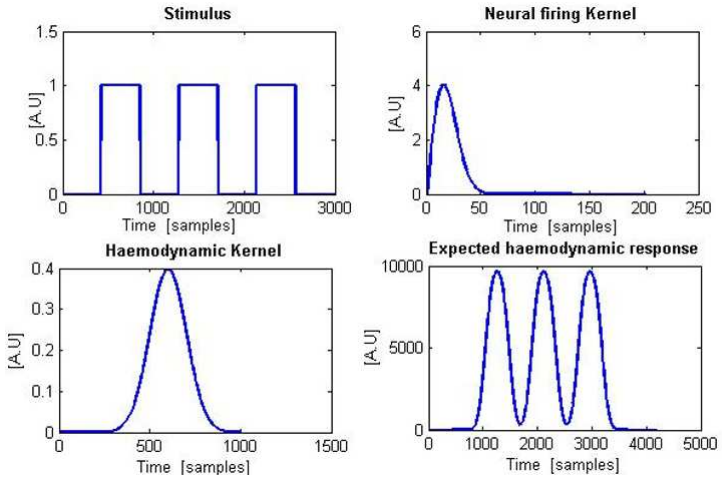


Figure 6.5: Expected hemodynamic response. The transformation from a stimulus train to an expected haemodynamic response of a single neural population assumed to fire with the stimulus. In this particular example the transformations have been achieved by convolution.

convolution. The expected haemodynamic response of the other channels is shown in 6.6 Again, in this example the four channels are responding to the stimulus. It would have been trivial to exemplify a brain region that would not respond to the stimulus (flat neural response) and or contaminate the channel behavior with stimulus locked or stimulus unlock additional information e.g. systemic, body movement, etc. However, with this example we only intend to show how the connectivity graph can be retrieved and thus we have avoid generating more elaborated synthetic data.

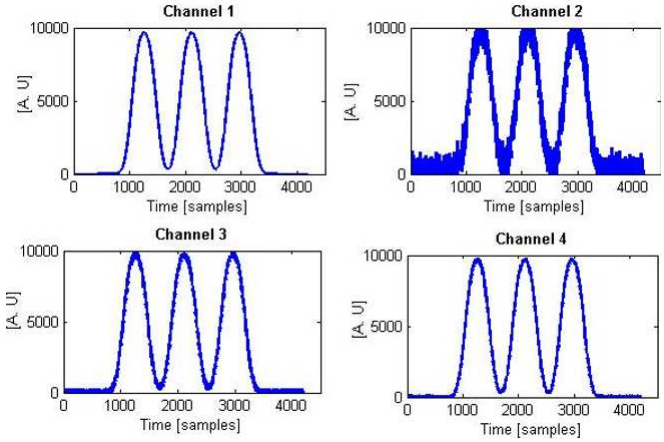


Figure 6.6: Expected a haemodynamic response of four channels from neuroimage.

### 6.4.2 Resolving the example

- Step 1) Projecting the neuroimage into an ambient space.
  Following the methodology afore described, the first step is to project each signal into a point in the Experimental space. In this example, we will use the simplest transformation to project a signal into a point; assuming that each sample of the signal is encoded along a different dimension, and that the value along such dimension is the signal amplitude at that particular sample. Of course, this is not necessarily an optimum decision. It is customary to think of $s[t]$ as a point $s =< s_1, \ldots, s_n >$ in a n dimensional space, where n is the number of samples. The value si along the $i-th$ dimension corresponds to the signal value or intensity at the $t-th$ sample; $s[t_i]$. In other words, there is a multivalued function $S : T \rightarrow R^n$ such that univocally makes a correspondence between sampled signals $s[t]$ and points in a space. Let $\delta_n$ be a function (of a coordinate system) representing the $n-th$ axis in $\mathbb{R}_{\ltimes}$. $\delta_n : Ts[n] \rightarrow R$ It is possible to construct a coordinate system $\nabla = S_n$ to project each sample to a coordinate and thus matching the signal to a point in the space.

- Step 2) Definition of the manifold
  The second step involves the imposition of a distance function which can elucidate the (dis)similarity among points in this space according to the brain function phenomenon of interest which in this case is assumed to be functional connectivity, and thus the distance function could be expected to characterize signal similarity. In its original proposition, Friston used 1-corr for this purpose. Mathematically, this is a pseudometric with known consequences but not being a metric complicates the mathematical discussion. Thus, and for no particular reason, in this example, we will opt for maintaining the ambient Euclidean metric as the distance function

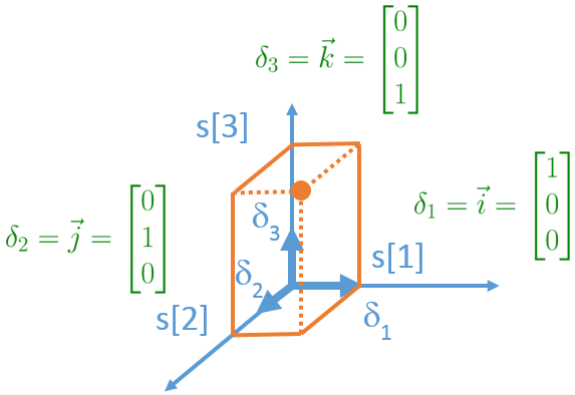


Figure 6.7: The point corresponding to a signal $s[t]$ in the space defined by the coordinate system $\delta_n$

encoding the phenomenon of interest. NOTE: Perhaps we are forcing things to be much simpler than they are in this example, as the particular choice of the Euclidean metric considering the specific encoding projection mentioned above is known to not be a good representative of signal similarity. Hopefully, we are allowed this license here. In this example each channel is considered a separate function $OC(t)$ and projects to distinct points, the whole neuroimage projects to a cloud of points in a 4191-dimensional space which for the sake of visualization it has been embedded here in 6.7 in a 2D space by means of Classical multidimensional scaling $(CMS)$.

In this example, considering that the synthetic signals have 4191 samples, the resulting ambient space is a 4191-dimensional space.

- Step 3) Definition of the solution to the brain phenomenon.
  Once the manifold is built, we still have to define what represents a solution to our problem of brain functional connectivity. As suggested above, in this case this can be easily afforded by having a given epsilon $\epsilon$ that expresses the minimum radius at which two points are to be considered functionally connected. Another well-known strategy to define the graph is basically considering a fixed number of neighbours with its own pros and cons. Of course, the choice of the epsilon is thresholding the adjacency matrix of the connectivity network. Let D be the matrix of pairwise distances among points. It is irrelevant whether in this case, and given that we have chosen a metric as a distance function the main diagonal of D is full of 0s and moreover D is symmetric. This has not need to be the case in pseudo-Riemannian manifolds e.g. causal manifolds. We can define our solution as the adjacency matrix resulting of pruning D for values above epsilon; Adjacency matrix = (D ¡ epsilon) Since in our synthetic dataset, all four channels

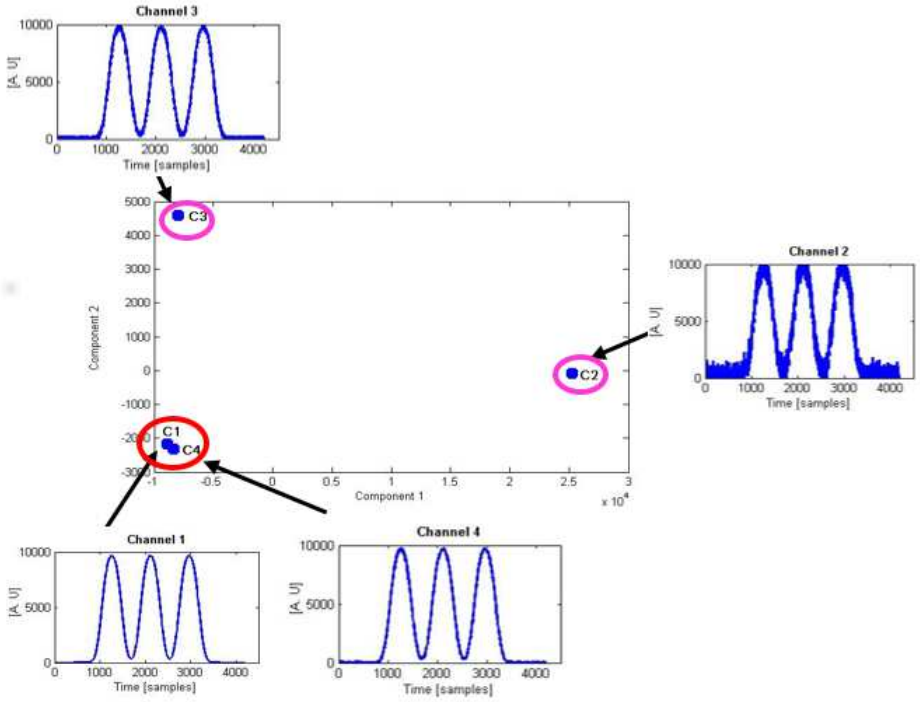


Figure 6.8: Manifold with cloud of points ordered (i.e. affected by a distance function). Point with most similar behavior (in this case less noise) are closer.

are responding actively to the stimulus, they all exhibit very similar behavior, and their only difference in this example lay in the amount of noise introduced. It can be appreciated in Figure 6 how the two with higher signal to noise ratio projects closer, whereas larger noise separates the points (note the different scale of the first and second CMS components in the figure). We can choose just to exemplify a non fully connected network, the choice of an epsilon = 1000AU. With this choice only channels 1 and 4 will be connected. Solutions in manifold based modelling do not have to be confined to graphs.

- Step 4) Renderization.
  Finally, the obtained graph can be represented in a more classical graph-based visualization. In this trivial example this is achieved effortlessly and the result is illustrated in Figure 6.9. Although in this case the graph is simple and undirected and moreover it does not contains cycles, more complicated manifold based modelling might yield also more complicated graphs.

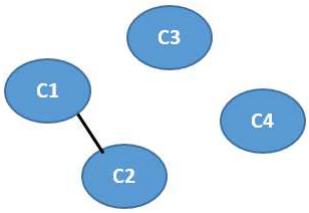


Figure 6.9: The solution graph. Channels C1 and C2 have high similarity according to the modelling choices made. With the chosen epsilon, the channels C3 and C4 there aren't functionally connected for us.

We have presented a very naive example of how manifolds can help to model brain function. It is convenient to emphasize that manifold based modelling of brain function is not constraint to the modelling decisions taken here, but instead it provides a rich framework for neuroimage analysis.

## 6.5 Conclusions

As progress of this first year, preliminary considerations about the modelling have been made and naive examples of the rationale behind some decisions have been exposed.

In this research we are hypothesizing that the brain function abides the topological construct of the manifold, and if that is the case, then many phenomena about brain function can be expressed under a topological framework. In other words, manifolds of different kinds are sufficiently expressive tools to hold solutions and predict observations across a range of brain behaviour phenomena. In this work we look forward to (i) produce some initial topological manifold-based models of different brain function phenomena, (ii) demonstrate some mathematical properties of such brain behaviour e.g. continuity of some specific model of brain haemodynamics, and (iii) make initial predictions of yet unseen observations, so that we provide foundational evidence of our hypothesis. This initial work aims to support the first two of these three targets. In particular,

- The preliminary simulation of the chain of transformations, even with naive kernels, help to understand the deformation suffered by the information as it flows through the system from the hidden variables of interest to the observable variables. Note however that optical image formation and reconstruction have not yet been simulated.

- The characterization of time signals and/or neuroimages as points or cloud of points in a space is an important step towards the manifold based modelling.

- The demonstration that the Euclidean distance is inadequate to capture signal

similarity by a simple counterexample, highlights the importance of setting the appropriate mathematical properties of the system.

The above preliminary advances allow claiming that manifold based modelling of effective connectivity appears to be a feasible endeavour. With huge potential to express many subanalysis e.g. by block, by treatment group, transversal o longitudinal, etc., as limited in section 6.2 by only dealing the encoding of the neuroimaging and the metric tensor on the manifold.

# Bibliography


Functional integration in the brain. In R. S. J. Frackowiak, K. J. Friston, C. D. Frith, R. J. Dolan, C. J. Price, S. Zeki, J. T. Ashburner, & W. D. Penny, editors, *Human Brain Function*, p. 971. Elsevier Academic Press, Burlington, 2nd edition, 2004.

L. F. Abbott & T. B. Kepler. Model neurons: From hodgkin-huxley to hopfield. In L. Garrido, editor, *Statistical mechanics of neural networks*, p. 5. Springer, 1990.

A. D. Aleksandrov, A. N. Kolmogorov, & M. A. Lavrent'ev. *Mathematics: its content, methods and meaning*. Dover, 2nd edition, 1999.

Simon R Arridge & Martin Schweiger. Image reconstruction in optical tomography. *Philosophical Transactions of the Royal Society B: Biological Sciences*, 352(1354):717–726, 1997.

V. Arsigny, P. Fillard, X. Pennec, & N. Ayache. Fast and simple calculus on tensors in the log-euclidean framework. In *Medical Image Computing and Computer-Assisted Intervention–MICCAI 2005*, p. 115. Springer, 2005.

L. A. Baccalá & K. Sameshima. Partial directed coherence: a new concept in neural structure determination. *Biol. cybern.*, 84(6):463, 2001.

D. S. Bassett & E. Bullmore. Small-world brain networks. *Neuroscientist*, 12(6):512, 2006.

M. F. Bear, B. W. Connors, & M. A. Paradiso. *Neuroscience: Exploring the brain*. Lippincott Williams & Wilkins, 3rd edition, 2007.

D Beeman. Hodgkin-huxley model. In D. Jaeger & R. Jung, editors, *Encyclopedia of computational neuroscience*, p. 1389. Springer-Verlag, New York (NY), 1st edition, 2014.

M. Berger & B. Gostiaux. *Differential geometry: manifolds, curves, and surfaces*, volume 115 of *Graduate Texts in Mathematics*. Springer-Verlag, 1st edition.

B. J. Biddle & M. M. Marlin. Causality, confirmation, credulity, and structural equation modeling. *Child Dev.*, 58(1):4, 1987.

L. Bombelli, J. Lee, D. Meyer, & R. D. Sorkin. Space-time as a causal set. *Phys. rev. lett.*, 59(5):521, 1987.

Gilberto Branco. *The development and evaluation of head probes for optical imaging of the infant head*. Phd thesis, University Collegue London, 2007.

C. Büchel & K. J. Friston. Modulation of connectivity in visual pathways by attention: cortical interactions evaluated with structural equation modelling and fmri. *Cereb. cortex*, 7(8):768, 1997.

E. Bullmore & O. Sporns. Complex brain networks: graph theoretical analysis of structural and functional systems. *Nat. Rev.Neurosci.*, 10(3):186, 2009.

R. B. Buxton, K. Uludağ, D. J. Dubowitz, & T. T. Liu. Modeling the hemodynamic response to brain activation. *Neuroimage*, 23:S220, 2004.

L. Cayton. Algorithms for manifold learning. Technical report, 2005.

F. Chamizo. Differential geometry bases, 2015. *https://www.uam.es/personal_pdi/ciencias/fchamizo/asignaturas/mgeom1516/ - mgeom1516.html*, Accessed 11-09-2015.

K. Çiftçi, B. Sankur, Y. P. Kahya, & A. Akın. Constraining the general linear model for sensible hemodynamic response function waveforms. *Med. & Biol. Eng. & Comput.*, 46(8):779, 2008.

P. Collier. *A most incomprehensible thing: notes towards a very gentle introduction to the mathematics of relativity, 2nd Edition*. Incomprehensible Books, 1st edition, 2012.

M. Cope & D. T. Delpy. System for long term measurement of cerebral blood and tissue oxygenation on newborn infants by near infrared transillumination. *Med. Biol. Eng. Comput.*, 26(3):289, 1988.

D. R. Cox & N. Wermuth. Causality: A statistical view. *Int. Stat. Rev.*, 72(3):285, 2004.

David T Delpy, Mark Cope, Pieter van der Zee, SR Arridge, Susan Wray, & JS Wyatt. Estimation of optical pathlength through tissue from direct time of flight measurement. *Physics in medicine and biology*, 33(12):1433, 1988.

S. G. Diamond, T. J. Huppert, V. Kolehmainen, M. A. Franceschini, J. P. Kaipio, S. R. Arridge, & D. A. Boas. Dynamic physiological modelling for functional diffuse optical tomography. *Neuroimage*, 30(1):88, 2006.

Solomon Gilbert Diamond, Katherine L. Perdue, & David A. Boas. A cerebrovascular response model for functional neuroimaging including dynamic cerebral autoregulation. *Math. Biosci.*, 220(2):102, 2009.

M.P. do Carmo. *Differential Geometry of Curves and Surfaces*. Prentice-Hall, 1st edition, 1976.

L. Dodero, H. Q. Minh, M. San Biagio, V. Murino, & D. Sona. Kernel-based classification for brain connectivity graphs on the riemannian manifold of positive definite matrices. In *IEEE 12th International Symposium on Biomedical Imaging (ISBI)*, p. 42. IEEE, 2015a.

L. Dodero, F. Sambataro, V. Murino, & D. Sona. Kernel-based analysis of functional brain connectivity on grassmann manifold. In N. Navab, J. Hornegger, W. M. Wells, & A. F. Frangi, editors, *Medical Image Computing and Computer-Assisted Intervention MICCAI 2015*, p. 604. 2015b.

M. Ferrari & V. Quaresima. A brief review on the history of human functional near-infrared spectroscopy (fnirs) development and fields of application. *Neuroimage*, 63 (2):921, 2012.

R. S. J. Frackowiak, K. J. Friston, C. D. Frith, R. J. Dolan, C. J. Price, S. Zeki, J. T. Ashburner, & W. D. Penny, editors. *Human brain function*. Elsevier Academic Press, 2nd edition, 2004.

K. J. Friston. Functional and effective connectivity in neuroimaging: a synthesis. *Hum. Brain Mapp.*, 2(1-2):56, 1994.

K. J. Friston, P. Fletcher, O. Josephs, A. Holmes, M. D. Rugg, & R. Turner. Event-related fmri: characterizing differential responses. *Neuroimage*, 7(1):30, 1998.

K. J. Friston, C. D. Frith, P. Fletcher, P. F. Liddle, & R. S.J Frackowiak. Functional topography: multidimensional scaling and functional connectivity in the brain. *Cereb. Cortex*, 6(2):156, 1996.

K. J. Friston, L. Harrison, & W. Penny. Dynamic causal modelling. *Neuroimage*, 19(4): 1273, 2003.

Karl J Friston. Functional and effective connectivity: a review. *Brain connectivity*, 1(1): 13–36, 2011.

Gerstner & Kistler. Hodgkin-huxley model, 2002. http://www.braininitiative.nih.gov/how.htm, Accessed 11-01-2016.

V Guillemin & A. Pollack. *Differential topology*, volume 370. AMS, Providence (RI), 1st edition, 2010.

F. B. Haeussinger, T. Dresler, S. Heinzel, M. Schecklmann, A. J. Fallgatter, & A.-C. Ehlis. Reconstructing functional near-infrared spectroscopy (fnirs) signals impaired by extra-cranial confounds: An easy-to-use filter method. *Neuroimage*, 95:69, 2014.

D. Heeger. Poisson model of spike generation, 2002. *http://neuro.bstu.by/ai/To-dom/My_research/Papers-2.1-done/ LIF/Feedforwardcopyfromelsewhere/B/Poisson-spiki-train/poisson.pdf*, Accessed 11-01-2016.

Javier Herrera-Vega & Felipe Orihuela-Espina. Image reconstruction in functional optical neuroimaging. the modelling and separation of the scalp blood flow: A research proposal. Technical Report CCC-15-002, Division of Computational Sciences. National Institute of Astrophysics, Optics and Electronics, INAOE (Mexico), Mar 2015.

N. J. Hicks. *Notes on differential geometry*. East-West Press, 1st edition, 1965.

B. Horwitz. The elusive concept of brain connectivity. *Neuroimage*, 19(2):466, 2003.

TJ Huppert, RD Hoge, SG Diamond, Maria Angela Franceschini, & David A Boas. A temporal comparison of bold, asl, and nirs hemodynamic responses to motor stimuli in adult humans. *Neuroimage*, 29(2):368–382, 2006.

M. Kamiński, M Ding, W. A. Truccolo, & S. L. Bressler. Evaluating causal relations in neural systems: Granger causality, directed transfer function and statistical assessment of significance. *Biol. cybern.*, 85(2):145, 2001.

M. J. Kaminski & K. J. Blinowska. A new method of the description of the information flow in the brain structures. *Biol. cybern.*, 65(3):203, 1991.

M. A. Kamran, M. Y. Jeong, & M. M. N. Mannan. Optimal hemodynamic response model for functional near-infrared spectroscopy. *Front. Behav. Neurosci.*, 9:151, 2015.

E. Kandel, J. Schwartz, T. Jessell, S. Siegelbaum, & A. J. Hudspeth. *Principles of neural science*. McGraw-Hill, 5th edition, 2000.

Takusige Katura, Naoki Tanaka, Akiko Obata, Hiroki Sato, & Atsushi Maki. Quantitative evaluation of interrelations between spontaneous low-frequency oscillations in cerebral hemodynamics and systemic cardiovascular dynamics. *Neuroimage*, 31(4): 1592–1600, 2006.

E. H. Kronheimer & R. Penrose. On the structure of causal spaces. 63(2):481, 1967.

V. R. Krym. Einstein equations on a 5-manifold with a causal structure in the absence of matter fields. *J. Math. Sci.*, 110(4):2841, 2002.

L. Lamport. Time, clocks, and the ordering of events in a distributed system. *Commun. ACM*, 21(7):558, 1978.

J. M. Lee. *Introduction to Smooth Manifolds*. Graduate Texts in Mathematics. Springer, 2nd edition, 2012. ISBN 9780387954486.

D. R. Leff, F. Orihuela-Espina, L. Atallah, A. Darzi, & G.-Z. Yang. Functional near infrared spectroscopy in novice and expert surgeons–a manifold embedding approach. In N. Ayache, S. Ourselin, & A. Maeder, editors, *Medical Image Computing and Computer-Assisted Intervention MICCAI 2007*, Lecture Notes in Computer Science, p. 270. Springer, Berlin (Heidelberg), 2007.

D. R. Leff, F. Orihuela-Espina, C. E. Elwell, T. Athanasiou, D. T. Delpy, A. W. Darzi, & G.-Z. Yang. Assessment of the cerebral cortex during motor task behaviours in adults: a systematic review of functional near infrared spectroscopy (fnirs) studies. *Neuroimage*, 54(4):2922, 2011.

Lynn H Loomis & Shlomo Sternberg. *Advanced calculus Revised edition*. Jones and Bartlett Publishers, Inc, 1968.

A. R. McIntosh & F. Gonzalez Lima. Structural equation modelling and its application to network analysis in functional brain imaging. *Human Brain Mapping*, 2:2–22, 1994.

JH Meek, CE Elwell, MJ Khan, J Romaya, JS Wyatt, DT Delpy, & S Zeki. Regional changes in cerebral haemodynamics as a result of a visual stimulus measured by near infrared spectroscopy. *P. Roy. Soc. B-Biol. Sci.*, 261(1362):351, 1995.

B. Ng, M. Dressler, G. Varoquaux, J.-B Poline, M. Greicius, & B. Thirion. Transport on riemannian manifold for functional connectivity-based classification. In *MICCAI - 17th International Conference on Medical Image Computing and Computer Assisted Intervention*, p. 405. Springer, 2014.

B. Ng, G. Varoquaux, J.-B. Poline, M. Greicius, & B. Thirion. Transport on riemannian manifold for connectivity-based brain decoding. *IEEE Trans. med. imaging*, 35(1): 208, 2015.

B. O'neill. *Semi-Riemannian Geometry With Applications to Relativity*, volume 103 of *Pure and applied mathematics*. Academic press, 1983.

F. Orihuela-Espina, D. R. Leff, D. R. James, A. W. Darzi, & G.-Z. Yang. Quality control and assurance in functional near infrared spectroscopy (fnirs) experimentation. *Phys. Med. Biol.*, 55(13):3701, 2010.

J. Pearl. Causal inference in statistics: An overview. *Statist. surv.*, 3:96, 2009.

M. Rainer. Cones and causal structures on topological and differentiable manifolds. *J. Math. Phys.*, 40(12):6589, 1999.

B. Rosengarten, O. Huwendiek, & M. Kaps. Neurovascular coupling and cerebral autoregulation can be described in terms of a control system. *Ultrasound Med. Bio.*, 27 (2):189, 2001.

A. Sassaroli & S. Fantini. Comment on the modified beer-lambert law. *Phys. med. biol.*, 49(14):N255, 2004.

F. Scholkmann, S. Kleiser, A. J. Metz, R. Zimmermann, J. P. Mata, U. Wolf, & M. Wolf. A review on continuous wave functional near-infrared spectroscopy and imaging instrumentation and methodology. *Neuroimage*, 85:6, 2014.

J Shawe-Taylor & N. Cristianini. *Kernel methods for pattern analysis*. Cambridge university press, 1st edition, 2004.

Sameer A Sheth, Masahito Nemoto, Michael Guiou, Melissa Walker, Nader Pouratian, & Arthur W Toga. Linear and nonlinear relationships between neuronal activity, oxygen metabolism, and hemodynamic responses. *Neuron*, 42(2):347–355, 2004.

Sameer A Sheth, Masahito Nemoto, Michael W Guiou, Melissa A Walker, & Arthur W Toga. Spatiotemporal evolution of functional hemodynamic changes and their relationship to neuronal activity. *Journal of Cerebral Blood Flow & Metabolism*, 25(7): 830–841, 2005.

S. Sra. Positive definite matrices and the symmetric stein divergence. Technical report, 2011.

Sungho Tak & Jong Chul Ye. Statistical analysis of fnirs data: a comprehensive review. *Neuroimage*, 85:72–91, 2014.

J. B. Tenenbaum, V. Dde Silva, & J. C. Langford. A global geometric framework for nonlinear dimensionality reduction. *Science*, 290(5500):2319, 2000.

J. A. Thorpe. *Elementary topics in differential geometry*. Springer-Verlag, 4th edition, 1994.

R. Toral, C. Masoller, C. R. Mirasso, M. Ciszak, & O. Calvo. Characterization of the anticipated synchronization regime in the coupled fitzhugh–nagumo model for neurons. *Physica A*, 325(1):192, 2003.

W. S. Torgerson. *Theory and methods of scaling*. Wiley, New York (NY), 1st edition, 1958.

G. Varoquaux, F. Baronnet, A. Kleinschmidt, P. Fillard, & B. Thirion. Detection of brain functional-connectivity difference in post-stroke patients using group-level covariance modeling. In T. Jiang, N Navab, & Viergever M. A. Pluim, J. P. W., editors, *Medical image computing and computer-assisted intervention–MICCAI 2010*, p. 200. Springer, 2010.

A. Villringer, J. Planck, C. Hock, L Schleinkofer, & U. Dirnagl. Near infrared spectroscopy (nirs): a new tool to study hemodynamic changes during activation of brain function in human adults. *Neurosci. lett.*, 154(1-2):101, 1993.

G. Zamora-López, C. Zhou, & J. Kurths. Exploring brain function from anatomical connectivity. *Front. Neurosci.*, 5:83.

Y. Zhang, D. H. Brooks, & D. A. Boas. A haemodynamic response function model in spatio-temporal diffuse optical tomography. *Phys. Med. Biol.*, 50(19):4625, 2005.